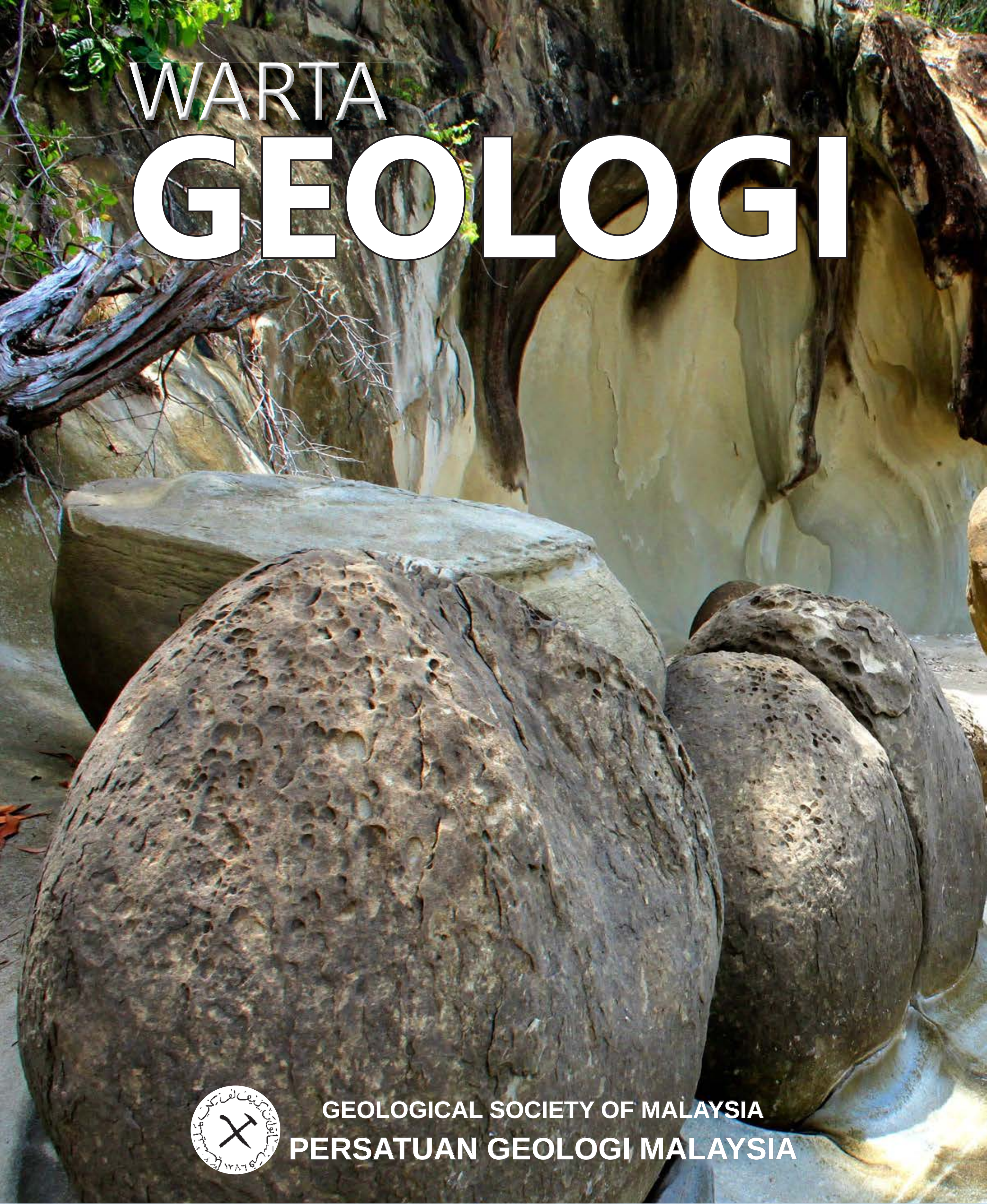

WARTA GEOLOGI

GEOLOGICAL SOCIETY OF MALAYSIA
PERSATUAN GEOLOGI MALAYSIA

Jilid 48 No. 1	April 2022	Volume 48 No. 1

ISSN 0126 - 5539; e-ISSN 2682 - 7549

PP2509/07/2013(032786) RM 80.00

PERSATUAN GEOLOGI MALAYSIA
Geological Society of Malaysia

The Geological Society of Malaysia (GSM) was founded in 1967 with the aim of promoting the advancement of geoscience, particularly in Malaysia and Southeast Asia. The Society has a membership of about 700 geoscientists based in Malaysia as well as abroad.

Warta Geologi is published three times yearly (April, August, December) by the Society. Warta Geologi publishes peer-reviewed short geological communications and original research on Earth Science. The scope includes local and regional geology, conservation geology, economic geology, engineering geology, environmental geology, geochemistry, geomorphology, geophysics, hydrogeology, palaeontology, petroleum geology, sedimentology, stratigraphy, structural geology and tectonics. Warta Geologi also reports on activities and news about GSM and the geoscience community in Malaysia.

Warta Geologi is distributed free-of-charge to members of the Society and is available free online through the Society's website: www.gsm.org.my.

GSM is committed to upholding standards of ethical behaviour at all stages of the publication process and we recommend the Committee on Publication Ethics (COPE) Best Practice Guidelines (http://publicationethics.org/resources/guidelines).

All articles published by Warta Geologi are licensed under the Creative Commons Attribution 4.0 International License. No fee is imposed on authors for publishing in the journal.

Further information can be obtained from:

The Editor,
Geological Society of Malaysia,
c/o Department of Geology, University of Malaya,
50603 Kuala Lumpur, Malaysia
Tel: 603-79577036 Fax: 603-79563900
Email: geologicalsociety@gmail.com

Warta Geologi

Cover photo: Coastal landscape at Batu Panjang, Kudat, Sabah. This photograph, taken by Joannes Muda, is the third-place winner of GSM National Geology Photography Competition 2020/2021.

DOI : https://doi.org/10.7186/wg481202201

Rock-soil transition in weathering of a porphyritic biotite granite

John Kuna Raj

No. 83, Jalan Burhanuddin Helmi 2, Taman Tun Dr. Ismail, 60000 Kuala Lumpur, Malaysia
Email address: jkr.ttdi.tmc@gmail.com

Abstract: Concentric layers of weathered materials around core-stones show the porphyritic biotite granite to experience sequential, but gradational, changes in visible features, textures and mineralogy as it transforms from 'rock' into 'soil'. The changes start with the opening-up of grain boundaries and micro-cracks (stage 1) followed by their dark brown staining (stage 2) and the subsequent alteration (to sericite and clay minerals) of groundmass plagioclase feldspar grains (stage 3). Biotite flakes are then bleached and altered (to chlorite and clay minerals) (stage 4) before there starts alteration (to sericite and clay minerals) of groundmass alkali feldspar grains (stage 5) and finally alteration (to sericite and clay minerals) of the alkali feldspar phenocrysts (stage 6). Quartz grains are not altered during these stages of weathering, but disaggregate and reduce in size due to continual opening-up of grain boundaries and micro-cracks. Increasing stages of weathering are marked by decreasing dry unit weights, dry densities and uniaxial compressive strengths, but increasing apparent porosities. The transition between 'rock' and 'soil' occurs during stage 6 when all plagioclase, and most alkali feldspar, groundmass grains have been altered as are some alkali feldspar phenocrysts. Stage 6 is marked by large apparent porosities (>18%) but low values of dry unit weight (<20.81 kN/m^3), dry density (<2,122 kg/m^3) and uniaxial compressive strength (<1.8 MPa).

Keywords: Porphyritic biotite granite, weathering, rock-soil transition

INTRODUCTION

The changes in mineralogy and texture that occur when rocks are weathered have been investigated with the aid of various chemical and petrological methods as well as laboratory index tests or assessed indirectly in the field (Bell, 2000). Several indices have been derived to quantify the changes in purely geological properties; some of them applied to correlate with, and indirectly determine, the engineering properties of weathered rock (Irfan, 1996). A review of the various methods used to characterize the weathering of rock is given in Martin & Hencher (1986) as well as Irfan (1996), and Bell (2000).

Several workers have applied essentially physical criteria to characterize the weathering of rock as Melton (1965) who used staining and friability of rock fragments to identify the degree of chemical weathering, and Ollier (1965) who proposed a similar scale based on friability alone to describe the weathering of granite. Onodera *et al.* (1974) used the number and width of micro-cracks as an index of the physical weathering of granite, while Uriel & Dapena (1978) proposed a void index to quantify the degree of physical weathering of granite. Iliev (1966) proposed a coefficient of weathering for granitic rock based on ultrasonic velocities in fresh, and weathered rock, whilst Irfan & Dearman (1978a) proposed a micro-petrographic index based on the ratio of primary to secondary minerals, micro-cracks and voids, to assess the grade of weathering of granite. After an extensive testing program, Irfan & Dearman (1978b) concluded that the quick absorption, Schmidt hammer, and point load strength, tests were reliable field tests for determination of a quantitative weathering index for granite. The main limitation in the use of such physical criteria to define the degree of weathering is that they can only be applied to material that is still sufficiently cohesive to be regarded as rock (Thomas, 1974).

Chemical analyses and calculation of various elemental, compound or molecular ratios, have also been widely used to define the state of weathering of rock material. Irfan (1996) applied several of these indices in the assessment of weathered granites in Hong Kong and concluded that the silica-to-alumina ratio as well as the Parker index (Parker, 1970) and the mobiles index (Irfan, 1996) were good indicators of the degree of weathering. Duzgoren-Aydin *et al.* (2002), however, applied thirty different chemical indices of weathering in their study of a weathering profile over crystal-vitric tuff in Hong Kong and concluded that application of these indices to directly scale changes in the physical state of rock material may not be warranted due to the complications involved.

0126-5539; 2682-7549 / Published by the Geological Society of Malaysia.

Duzgoren-Aydin & Aydin (2006) in a comprehensive re-assessment of chemical weathering indices for felsic igneous rocks in Hong Kong furthermore, concluded that chemical weathering indices were not be as useful in determining weathering grades as was originally thought, though they could be used as tools to detect chemical heterogeneities.

In weathering profiles over granite, different stages of weathering of rock material are often present at similar depths, as in the concentrically developed stages of weathering around core-stones and core-boulders (Dearman, 1974). Dearman (1976), and Lee & de Freitas (1989), have thus, emphasized the need to differentiate between "weathering of rock material" and "weathering of rock mass". Martin & Hencher (1986) have also pointed out that weathering profiles are characterized by heterogeneous earth materials at various stages of decomposition and/or disintegration as weathering processes are rarely sufficiently uniform to give gradual and predictable changes in mineralogical and textural properties.

In an earlier publication Raj (1985) has described the characterization of the weathering profile developed over porphyritic biotite granite at Km 31 of the Kuala Lumpur - Karak Highway. In the publication, Raj (1985) briefly described the different stages of weathering of bedrock that developed around core-stones and core-boulders, and that extended inward from discontinuity planes in the bedrock mass. In this short note, the concentric rings of weathered materials around core-stones are further discussed in order to define more clearly the transition between 'rock' and 'soil' in the weathering of the porphyritic biotite granite.

METHODOLOGY

Several core-stones were first collected from the weathering profile over porphyritic biotite granite at Km 31 of the Kuala Lumpur - Karak Highway (Figure 1). These litho-relicts were taken to the laboratory where they were diamond-sawn into slabs of variable thicknesses. The concentric rings of weathered materials around the rims of the slabs were then examined with a hand lens to identify differences in visible features as staining, colour, texture

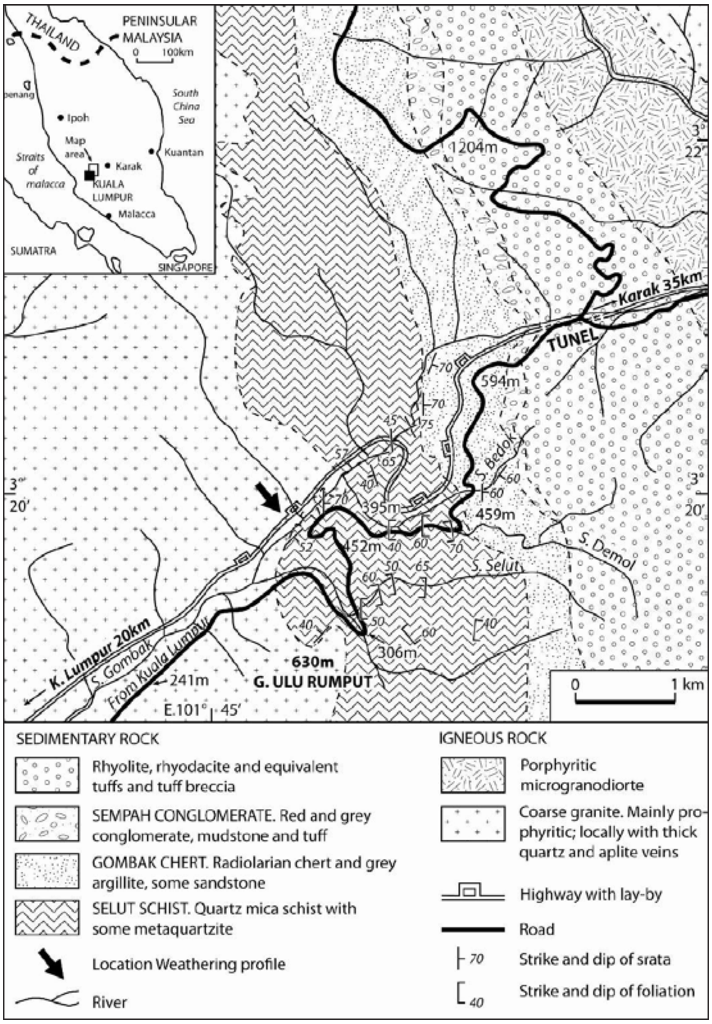

Figure 1: Geology Map of Genting Sempah area, Pahang & Selangor (Haile *et al*., 1977).

and appearance of mineral grains. The extent of alteration of feldspar phenocrysts and groundmass grains was also determined following the method of Irfan & Dearman (1978b) (Table 1). Thin-sections were then prepared of the concentric rings of weathered materials and a petrological microscope used to identify changes in texture and mineralogy of the phenocrysts and groundmass grains.

Variations in visible features as well as textural and mineralogical changes were then used to define different stages of weathering of the granitic bedrock. This procedure of identifying different stages of weathering follows that of earlier workers as Ruxton & Berry (1957) who defined stages of weathering of granitic rock material in terms of staining and alteration of mineral grains as well as the friability of material. Baynes *et al.* (1978), Irfan & Dearman (1978a) and Dearman *et al.* (1978) furthermore, have adopted a similar procedure to define different stages of weathering of granite in southwest England on the basis of separate assessments of the effects of physical disintegration and chemical decomposition.

Small tetrahedral blocks of the different stages of weathering were also sawn-out from the slabs and their unit weights, densities and apparent porosities determined by the saturation and buoyancy method of ISRM (1979). Several of these tetrahedral blocks were also loaded to failure in a compression machine following standard procedure in order to determine uniaxial compressive strengths (ISRM, 1981).

GEOLOGICAL SETTING

The weathering profile at the slope cut at Km 31 of the Kuala Lumpur – Karak Highway is developed over porphyritic biotite granite (Figure 1). This bedrock forms part of the eastern lobe of the Late Triassic (199-210 Ma) Kuala Lumpur Granite (Ng, 1992) and has given rise to a fluvially dissected, hilly to mountainous terrain of steep slopes and narrow, deep valleys. The bedrock continues to outcrop to the west over a distance of about 10 km, but to the east, is in contact with a sequence of schists, and sedimentary and volcanic rocks, that occur as a roof pendant within the Main Range Granite (Haile *et al.*, 1977). The granitic bedrock is strongly jointed and cut by a number of moderately to steeply dipping faults of variable strike. A number of epidote and quartz feldspar veins with tourmaline as well as aplite and leucocratic microgranite dykes are also seen within the bedrock.

The grey bedrock is medium to coarse grained and usually porphyritic with large alkali feldspar phenocrysts (up to 4 cm in length). The essential minerals are quartz, alkali feldspar, plagioclase feldspar and biotite, whilst the accessory minerals include apatite, tourmaline and zircon. Quartz occurs as anhedral crystals, filling interstices in the groundmass and sometimes forms small phenocrysts. The alkali feldspars include microcline, orthoclase and perthites, and occur both as phenocrysts and as fine to medium grained crystals in the groundmass. The alkali feldspars sometimes contain quartz, biotite and plagioclase inclusions. The plagioclase feldspars, of an albite to andesine composition, are usually found as euhedral to subhedral, fine to medium grained crystals in the groundmass and are often sericitized. The biotites occur as fine to medium grained, generally euhedral crystals and are found both as disseminated grains and as aggregates within the bedrock material. Close to the faults, hydrothermal alteration of the plagioclase feldspar and biotite grains has occurred.

RESULTS

Stages of weathering

Variations in visible features as well as textural and mineralogical changes allowed differentiation of six generalized stages of weathering of the porphyritic biotite granite (Tables 2 and 3). These stages of weathering, as illustrated in Plate 1, start with the opening-up of grain boundaries and micro-cracks (stage 1) followed by their dark brown staining with secondary iron oxides and hydroxides (stage 2). The groundmass plagioclase feldspar grains then start to alter (to sericite and clay minerals) (stage 3) before there is bleaching and alteration (to chlorite and clay minerals) of biotite flakes (stage 4). There is then the alteration (to sericite and clay minerals) of the groundmass alkali feldspar grains (stage 5) before there starts alteration (to sericite and clay minerals) of alkali feldspar phenocrysts (stage 6). Quartz grains are not altered

Table 1: Extent of alteration of feldspar grain (after Irfan & Dearman, 1978b). (Material from probed feldspar grain rubbed between thumb and finger).

Feel	Description	Interpretation
Gritty	Partially decomposed	Feldspar grain altered to sericite & clay along micro-fracture & cleavage planes only
Powdery (Silky)	Completely decomposed	Feldspar grain entirely altered to mainly sericite & some clay
Clayey	Completely decomposed	Feldspar grain entirely altered to clay & some sericite

during these stages of weathering, but do disaggregate and reduce in size due to the continual opening-up of grain boundaries and micro-cracks.

Physical properties of different stages of weathering

Physical properties of samples from the different stages of weathering are gradational in nature though there are some differences between stages (Table 4). Unaltered (stage 0), and stage 1 weathered, bedrock material is characterized by large dry unit weights (>25.63 kN/m^3) and dry density (>2,613 kg/m^3), but low apparent porosities (<2.1%). Stage 6 weathered bedrock material, however, is characterized by relatively low dry unit weights (<20.81 kN/m^3) and dry density (<2,122 kg/m^3), but large apparent porosities (>18.4%).

Table 2: Stages of weathering of the porphyritic biotite granite.

Stage	Hand specimen description	Thin-section description
6	Yellowish 'rock' material with open grain boundaries & micro-cracks. Some brown stains. Groundmass feldspar grains all appear altered (gritty to clayey). Some feldspar phenocrysts altered (powdery to gritty). Quartz grains & some feldspar phenocrysts appear unaltered. 'Rock' material has weak fabric & can disaggregate when dry samples are agitated in water.	All groundmass plagioclase & alkali feldspar grains are altered (to sericite & clay minerals). A few alkali feldspar phenocrysts are similarly altered. Biotite flakes all appear altered (to sericite & clay minerals). Quartz grains appear unaltered. Grain boundaries & micro-cracks are all open.
5	Yellowish rock material with brown stains along some grain boundaries & micro-cracks. Stains prominent close to bleached biotite flakes. Quartz grains & alkali feldspar phenocrysts appear unaltered. Groundmass feldspar grains (≈50% of all feldspars) are altered, yellow & gritty to powdery.	Brown stains along grain boundaries & micro-cracks, often extending out from altered biotite flakes. All plagioclase, & most alkali feldspar, groundmass grains are altered (to sericite & clay minerals). Quartz & alkali feldspar phenocrysts appear unaltered. Grain boundaries & micro-cracks are open.
4	Brownish grey rock material with brown stains along grain boundaries & micro-cracks. Most essential mineral grains appear unaltered with vitreous to sub-vitreous lustres. Many feldspar grains (≈30% of all feldspars) are white to yellow & gritty.	Brown stains along most grain boundaries & micro-cracks. Most essential mineral grains appear unaltered. Most groundmass plagioclase grains are altered (to sericite & clay minerals). Some bleached biotite flakes. Many open grain boundaries & micro-cracks.
3	Dark brownish grey rock material. Brown stains along grain boundaries & micro-cracks. Essential mineral grains appear unaltered with vitreous to sub-vitreous lustres. Some feldspar grains (≈10% of all feldspars) are white to yellow & gritty.	Brown stains along most grain boundaries & micro-cracks. Most essential mineral grains appear unaltered. Many groundmass plagioclase grains are altered (to sericite & clay minerals). Many open grain boundaries & micro-cracks.
2	Brownish grey rock material. Brown stains along some grain boundaries. Essential mineral grains appear unaltered with vitreous to sub-vitreous lustres.	Brown stains along some open grain boundaries & micro-cracks. Essential mineral grains appear unaltered except for several sericitized plagioclase grains.
1	Grey rock material. Essential mineral grains appear unaltered with vitreous to sub-vitreous lustres. Some open micro-cracks.	Essential mineral grains are unaltered. A few sericitized plagioclase grains. A few open grain boundaries & micro-cracks.
0	Grey rock material. Essential mineral grains (quartz, biotite, alkali feldspar & plagioclase) unaltered with vitreous to sub-vitreous lustres. (Unweathered).	Essential mineral grains (quartz, biotite, alkali feldspar & plagioclase) are unaltered. A few sericitized plagio-clase grains. Tight grain boundaries & micro-cracks.

Table 3: Variations in visible features, textures and mineralogy during weathering.

Stage	Grain boundaries & micro-cracks	Essential (Primary) Minerals						Secondary Minerals	
		Ground-mass Plagio-clase	Alkali Feldspar		% Felspar Grains Altered	Biotite	Quartz	Silt Size (Sericite)	Clay Size
			Ground-mass	Pheno-crysts					
6	Most open with yellow stains	All altered	All altered	A few altered	≈70%	All altered	Unaltered	Abundant	Some
5	Some open with brown stains	All altered	Most altered	Unaltered	≈50%	Many altered	Unaltered	Many	A few
4	Most open with brown stains	Most altered	Some altered	Unaltered	≈30%	Some altered	Unaltered	Some	A few
3	Many open with brown stains	Some altered	Unaltered	Unaltered	≈10%	Fresh	Unaltered	A few	A few
2	Some open with brown stains	Unaltered	Unaltered	Unaltered	0%	Unal-tered	Unaltered	A few	None
1	A few open. No stains	Unaltered	Unaltered	Unaltered	0%	Unal-tered	Unaltered	A few	None
0	Tight. No stains	Unaltered	Unaltered	Unaltered	0%	Unal-tered	Unaltered	A few	None

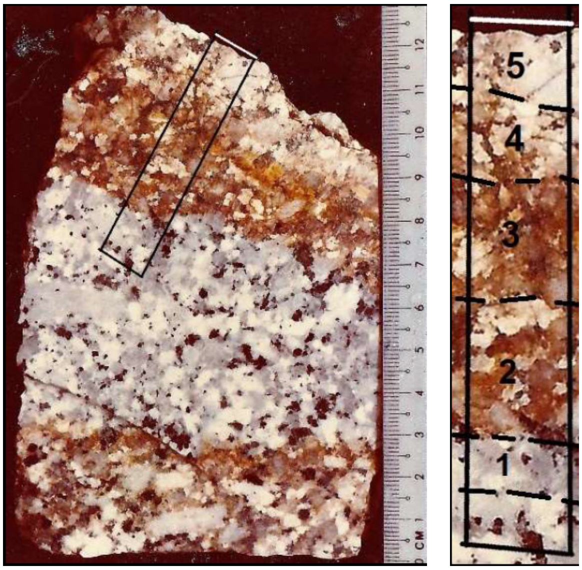

Plate 1: Weathering stages 1 to 5 around core-stone.

Table 4: Physical properties of different stages of weathering.

Sample Number	Stage of Weathering	Dry Unit Weight (kN/m^3)	Dry Density (kg/m^3)	Apparent Porosity (%)
A1	0	25.71	2,621	1.8
A2	0	25.65	2,615	2.1
A3	0	25.90	2,641	1.1
A4	0	25.95	2,646	0.9
A5	1	25.65	2,615	2.1
A6	1	25.63	2,613	2.1
A7	2	25.37	2,586	2.4
A8	2	25.34	2,584	2.5
A9	2	25.14	2,564	3.5
A10	2	25.30	2,580	3.0
A11	3	23.64	2,411	8.3
A12	3	23.83	2,430	7.6
A13	3	24.48	2,496	5.8
A14	3	24.60	2,508	5.4
A15	3	24.31	2,479	6.5
A16	3	23.96	2,443	7.8
A17	4	22.91	2,336	12.2
A18	4	22.83	2,328	12.5
A19	4	22.63	2,307	12.9
A20	4	22.68	2,313	12.4
A21	4	22.38	2,282	12.6
A22	4	22.50	2,294	12.4
A23	5	22.00	2,243	14.7
A24	5	21.90	2,233	15.1
A25	5	21.93	2,236	14.3
A26	5	21.80	2,223	15.2
A27	5	21.95	2,238	14.2
A28	5	21.98	2,241	14.5
A29	6	20.61	2,101	19.2
A30	6	20.73	2,114	19.0
A31	6	20.81	2,122	18.4
A32	6	19.86	2,025	21.8
A33	6	19.50	1,988	20.7

Stages 2 to 5 weathered bedrock bedrock material furthermore, show intermediate and decreasing values of dry unit weight and dry density, but increasing values of apparent porosity (Table 4). Stages 2, 3, 4 and 5 weathered, bedrock material are thus characterized by dry unit weights ranging from 25.14-25.37 kN/m^3 through 23.64-24.60 kN/m^3 and 22.38-22.91 kN/m^3 to 21.95-22.00 kN/m^3, respectively. Their corresponding dry densities range from 2,564-2,586 kg/m^3, through 2,411-2,508 kg/m^3 and 2,282-2,336 kg/m^3 to 2,223-2,243 kg/m^3, respectively. Values of apparent porosity decrease distinctly from stages 2 through 3 and 4 to 5 with values of 2-4 %, 5-9%, 12-13% and 14-16%, respectively.

Uniaxial compressive strength

Samples of the different stages of weathering show gradational changes in uniaxial compressive strengths, though there are differences between the various stages (Table 5). Unaltered (stage 0), and stage 1 weathered, porphyritic biotite granite is characterized by large uniaxial compressive strengths (>94.1 MPa), whilst stage 6 weathered bedrock material is characterized by very low strengths (<1.8 MPa).

Stages 2 to 5 weathered bedrock bedrock material furthermore, show intermediate, but decreasing values of uniaxial compressive strength (Table 5). Stages 2, 3, 4 and 5 are thus characterized by uniaxial compressive strengths ranging from 53.5-67.6 MPa through 22.2-46.1 MPa and 7.5-14.5 MPa, to 3.2-4.6 MPa, respectively.

DISCUSSION

As weathering proceeds, a 'rock' material will become increasingly decomposed and/or disintegrated until ultimately a 'soil' is formed (Bell, 2000). The terms 'rock' and 'soil' material have been defined in various ways, though for geotechnical purposes, the best definitions are those by Terzaghi & Peck (1948). Terzaghi & Peck (1948, p. 4) have simply defined 'soil' as being "a natural aggregate of mineral grains that can be separated by such gentle means as agitation in water", whilst 'rock' would not be able to be so separated.

In the reduction process of a rock to a soil, various stages can be recognized, though it is almost inevitable that the boundaries between the stages are gradational (Bell, 2000). This has been shown in the present study where six sequential, but gradational, changes in visible features, textures and mineralogy can be differentiated in the concentric rings of weathered materials formed around core-stones of the porphyritic biotite granite (see Section 4.1).

Stage 6 weathered bedrock material represents the transition between rock and soil material for it comprises natural aggregates that can be disaggregated when dry specimens are agitated in water (Table 2). In this stage, almost all the plagioclase, and most alkali feldspar, groundmass grains have been altered (to sericite and clay minerals) as are a few alkali feldspar phenocrysts (Table 3). Strong bonds between individual mineral grains that existed in the earlier stages of weathering are thus no longer present in the stage 6 weathered bedrock material. Alteration of the groundmass feldspar grains has thus led to the loss of bonds between individual grains.

The rock - soil transition furthermore, is gradational in nature as shown by differences in the physical properties of samples from stage 6 weathered bedrock material (Table 4) and the decreasing uniaxial compressive strengths (Table 5). Interestingly enough, the samples from stage 6 weathered bedrock material samples with their low uniaxial compressive strengths (<1.8 MPa) would be classified as extremely weak to weak rock materials in existing classifications of earth materials as those by ISRM (1983) and IAEG (1989).

CONCLUSION

Concentric rings of weathered materials developed around core-stones show the porphyritic biotite granite to experience sequential, but gradational, changes in visible features, textures and mineralogy as it transforms from 'rock' into 'soil'. The changes start with the opening-up of grain boundaries and micro-cracks (stage 1) followed by their dark brown staining (stage 2) and the subsequent alteration (to sericite and clay minerals) of groundmass plagioclase feldspar grains (stage 3). Biotite flakes are then bleached and altered (to chlorite and clay minerals) (stage 4) before there starts alteration (to sericite and clay minerals) of groundmass alkali feldspar grains (stage 5) and finally alteration (to sericite and clay minerals) of alkali feldspar phenocrysts (stage 6). Quartz grains are not altered during these stages of weathering, but disaggregate and reduce in size due to continual opening-up of grain boundaries and micro-cracks. Increasing stages of weathering are marked by decreasing dry unit weights, dry densities and uniaxial compressive strengths, but increasing apparent porosities. The transition between 'rock' and 'soil' occurs during stage 6 when all plagioclase, and most alkali feldspar, groundmass grains have been altered as have been some alkali feldspar phenocrysts. Stage 6 weathered bedrock material is characterized by large apparent porosities (>18%) but low values of dry unit weight (<20.81 kN/m^3) and dry density (<2,122 kg/m^3) as well as low uniaxial compressive strengths (<1.8 MPa).

ACKNOWLEDGEMENTS

Grateful thanks are extended to the University of Malaya for an F-Vote research grant that provided financial assistance for fieldwork involved in preparation of this article. Grateful thanks are also extended to the two anonymous reviewers for their valuable comments.

Table 5: Uniaxial compressive strength of different stages of weathering.

Sample Number	Stage of weathering	Uniaxial Compressive Strength (MPa)
B1	0	174.30
B2	0	151.10
B3	0	128.30
B4	1	101.30
B5	1	94.10
B6	2	67.70
B7	2	53.50
B8	3	46.10
B9	3	44.79
B10	3	37.41
B11	3	29.85
B12	3	26.65
B13	3	22.21
B14	4	14.50
B15	4	11.48
B16	4	10.04
B17	4	9.26
B18	4	8.11
B19	4	7.52
B20	5	4.56
B21	5	4.40
B22	5	4.29
B23	5	3.93
B24	5	3.66
B25	5	3.18
B26	6	1.82
B27	6	1.79
B28	6	1.48
B29	6	1.42
B30	6	0.82
B31	6	0.29

CONFLICT OF INTEREST

The author has no conflicts of interest to declare that are relevant to the content of this article.

REFERENCES

Baynes, F.J., Dearman, W.R. & Irfan, T.Y., 1978. Practical assessment of grade in a weathered granite. Bulletin International Association Engineering Geology, 18, 101-109.

Bell, F.G., 2000. Engineering properties of soils and rocks. Blackwell Science Ltd., Oxford. 482 p.

Dearman, W.R., 1974. Weathering classification in the characterization of rock for engineering purposes in British practice. Bulletin International Association Engineering Geology, 9, 33-42.

Dearman, W.R., 1976. Weathering classification in the characterization of rock: A revision. Bulletin International Association Engineering Geology, 13, 123-127.

Dearman, W.R., Baynes, F.J. & Irfan, T.Y., 1978. Engineering grading of weathered granite. Engineering Geology, 12, 345-374.

Duzgoren-Aydin, N.S., Aydin, A. & J. Malpas, 2002. Re-assessment of chemical weathering indices: Case study on pyroclastic rocks of Hong Kong. Engineering Geology, 63, 99-110.

Duzgoren-Aydin, N.S. & A. Aydin, 2006. Chemical and mineralogical heterogenities of weathered igneous profiles: Implications for landslide investigations. Natural Hazards & Earth System Sciences, 6, 315-322.

Haile, N.S., Stauffer, P.H., Krishnan, D., Lim, T.P. & Ong, G.B., 1977. Palaeozoic redbeds and radiolarian cherts: Reinterpretation of their relationships in the Bentong and Raub areas, West Pahang, Peninsular Malaysia. Bulletin of the Geological Society of Malaysia, 8, 45-60.

IAEG, International Association Engineering Geology, 1981. Rock and soil description for engineering geological mapping. Bulletin International Association of Engineering Geology, 24, 235-274.

Iliev, I.G., 1966. An attempt to estimate the degree of weathering of intrusive rocks from their physico-mechanical properties. Proceedings 1st International Congress Rock Mechanics, Lisbon, 25 Sept - 1 Oct, 1966. 1, 109-114.

Irfan, T.Y. & Dearman, W.R., 1978a. Engineering classification and index properties of a weathered granite. Bulletin International Association Engineering Geology, 17, 79-90.

Irfan, T.Y. & Dearman, W.R., 1978b. The engineering petrography of a weathered granite in Cornwall, England. Quarterly Journal Engineering Geology, 11, 233-244.

Irfan, T.Y., 1996. Mineralogy and fabric characterization and classification of weathered granitic rocks in Hong Kong. Geo Report No. 41, Geotechnical Engineering Office, Civil Engineering Department, Hong Kong. 159 p.

ISRM (International Society for Rock Mechanics), 1979. Suggested methods for determining water content, porosity, density, absorption and related properties and swelling and slake durability index properties. International Journal Rock Mechanics Mineral Science & Geomechanics Abstracts, Abstracts, 16, 141-156.

ISRM (International Society of Rock Mechanics), 1981. Suggested methods for determining the uniaxial compressive strength and deformability of rock materials. In: Brown, E.T., (Ed.), Rock characterization, testing and monitoring. International Society Rock Mechanics, Pergamon Press, 111-116.

Lee, S.G. & de Freitas, M.H., 1989. A revision of the description and classification of weathered granite and its application to granites in Korea. Quarterly Journal Engineering Geology, 22, 31-48.

Martin, R.P. & Hencher, S., 1986. Principles for description and classification of weathered rock for engineering purposes. Geological Society of London, Engineering Geology Special Publication 2, 299-308.

Melton, M.A., 1965. The geomorphic and paleoclimatic significance of alluvial deposits in Southern Arizona. Journal of Geology, 73, 1-38.

Ng, T.F., 1992. Petrography, structure and geotechnical studies of the Kuala Lumpur Granite, eastern part of Kuala Lumpur, Peninsular Malaysia. (Unpublished) M.Phil. Thesis. Institute of Advanced Studies, University of Malaya, Kuala Lumpur. 527 p.

Ollier, C.S., 1965. Some features of granite weathering in Australia. Zeischt Geomorfologie, 9, 285-304.

Onodera, T.F., Yoshinaka, R. & Oda, M., 1974. Weathering and its relation to mechanical properties of granite. Proceedings 3rd Congress, International Society Rock Mechanics, Denver, 2, 71-78.

Parker, A., 1970. An index of weathering for silicate minerals. Geological Magazine, 107, 501-504.

Raj, J.K., 1985. Characterization of the weathering profile developed over a porphyritic biotite granite bedrock in Peninsular Malaysia. Bulletin International Association Engineering Geology, 32, 121-128.

Ruxton, B.P. & Berry, L., 1957. The weathering of granite and associated erosional features in Hong Kong. Bulletin Geological Society of America, 68, 1263-1292.

Terzaghi, K. & Peck, R.B., 1948. Soil mechanics in engineering practice. John Wiley and Son Inc., USA. 566 p.

Thomas, M.F., 1974. Tropical geomorphology - A study of weathering and landform development in warm climates. Macmillan Press Ltd., London. 332 p.

Uriel, S. & Dapena, E., 1978. Influence of weathering on the mechanical properties of granitic rocks. Proceedings 3rd International Congress, International Association of Engineering Geology, Madrid, 1, 91-104.

Manuscript received 4 September 2021;
Received in revised form 11 January 2022;
Accepted 13 January 2022
Available online 26 April 2022

DOI : https://doi.org/10.7186/wg481202202

Groundwater exploration using vertical electrical sounding and 2D electrical resistivity tomography in shale formation: A case study of Sabongida, Plateau State, North Central Nigeria

Solomon Nehemiah Yusuf[1,*], Hilnan Christopher Drenkat[1], Charity Mamza Azi[2]

[1] Department of Geology, University of Jos, Bauchi Road, 930105, Jos, Plateau State, Nigeria
[2] Department of Geology, Nasarawa State University, 911019, Keffi, Nasarawa State, Nigeria
* Corresponding author email address: yusufso@unijos.edu.ng

Abstract: Sabongida is characterized by lots of abortive boreholes which are often shallow as a result of the complex nature of shale formation in the area and limited application of integrated geophysical techniques before drilling of boreholes. The presence of shale formation in the area makes it extremely difficult to drill productive boreholes, while the existing hand dug wells are always shallow due to the difficulty in digging deeper wells, this and other factors motivated the choice of the study location for the purpose of proffering solutions to solve the perennial water problem in the area. Twenty-two (22) vertical electric soundings data (VES) using Schlumberger array with the aid of Ohms mega resistivity meter were conducted with electrode spread of AB/2 = 215 m and eleven (11) 2D electrical resistivity tomography data (ERT) using ADMT – 600 S - X equipment were acquired. ERT was conducted using 20 m as the length of each profile with 300 m in 10 profile lines and 400 m as the depth of probing. The result of the VES interpretation shows three to five geo-electric layers while the geo-electric section revealed the aquifers to consist of sandstones with varying thicknesses. Two groundwater potential zones were delineated as shelly sandstones and clayey sand. The different color band indicates the different layers within the ground as the soil resistivity varies, blue indicates low resistivity values, green - yellow indicates moderate resistivity values while high resistivity values are brown - red. The results from the 2D images indicate the low resistivity regions, suggesting aquifer is within the depths of 150 to 300 m. Thus, the recommended depths for drilling of productive boreholes are 180 to 210 m and 270 to 300 m in Sabongida.

Keywords: Electrical, resistivity, 2D, tomography, shale, aquifer, water scarcity

INTRODUCTION

Groundwater has undoubtedly gained increased recognition in developing parts of the world today. Groundwater availability is determined by the presence of hydraulic qualities of groundwater bearing units, while portability is determined by hydrogeochemical properties and contamination/pollution vulnerability (Obiadi *et al*., 2016). Water is regarded to be a necessary resource for survival; hence its significance cannot be overstated. It is however disturbing if this all-important resource is becoming more and more scarce or difficult to explore (Christopher, 2006). According to Rosen & Vincent, 2014, water scarcity is especially acute in developing countries, where figures suggest that 67 % of the rural population lacks access to safe drinking water. This is due to the fact that people in rural regions rely on surface water from lakes, streams, ponds, and rivers to survive. Surface water bodies, on the other hand, are unreliable due to high evaporation rates, which are common in high temperate regions, and they are often polluted and infected with waterborne diseases (Gyau-Boakye *et al*., 2008). Treatment is required to supply water from these sources, primarily for home use, especially in small towns (Rosen & Vincent, 2014). People in impoverished regions who cannot afford such treatment utilize the waters as they are, resulting in epidemics of water-borne diseases including diarrhea, guinea worm infestation and bilharzia.

Due to the fact that groundwater is difficult to locate, a range of geophysical methods complimenting each other are required to offer data on its occurrence and location. Thapa *et al*. (2008) proposed that many criteria such as lithology, slope, lineaments, hydro geomorphology, land use and land cover should be understood in order to estimate groundwater potential zones of a region. Soil information is also crucial for determining groundwater potential zones. Coarse soils, for example, are generally permeable, but fine-grained soils have a lower permeability (Amaresh *et al*., 2006).

0126-5539; 2682-7549 / Published by the Geological Society of Malaysia.

Geophysics can be used to map groundwater resources as well as assess water quality (Hewaidy *et al*., 2015). Gravity, magnetics, seismic, electrical resistivity, electrical resistivity tomography, and electromagnetic approaches are just a few of the geophysical techniques that have been used to prospect for groundwater (Reynolds, 1997). The electrical and electromagnetic surveys have shown to be very useful in groundwater studies by Soupios *et al*. (2005). This is because many geological formation attributes that are important in hydrogeology, such as porosity and permeability of rocks, may be linked to electrical resistivity and conductivity signatures. Many of these geophysical approaches have since been employed to characterize groundwater, but the electrical method has once again proven to be the most successful (Eke & Igboekwe, 2011). This is why this study seeks to use the vertical electric sounding (VES) and 2D electric resistivity tomography in the search for groundwater potential zones in a predominantly shale formation in Sabongida, Langtang South Local Government Area of Plateau State, Nigeria.

In groundwater resource mapping, geophysical techniques are used for mapping out subsurface geological structure in which groundwater occurs (Araffa, 2012). Sabongida is characterized by lots of abortive boreholes which are often shallow as a result of the complex nature of geology of the area due to the presence of shale formation and, limited application of integrated geophysical techniques before drilling of boreholes. The presence of shale formation in the area makes it extremely difficult to drill productive boreholes while the hand dug wells are always shallow due to difficulties in penetrating the shale formation. Based on Soupios *et al*. (2005) and Ekwe *et al*. (2006), the vertical electrical sounding (VES) approach has been effectively employed in groundwater exploration and the computation of hydraulic properties such as hydraulic conductivity and transmissivity, with very effective and efficient results. Ojo *et al*. (2007) stated that the use of vertical electrical sounding (VES) technique has proven to be useful in achieving good lateral coverage for mapping aquifer units and drilling productive boreholes. (Onimisi *et al*., 2013) used electrical resistivity surveys to identify and locate good groundwater potential area. According to Igboekwe (2005) and Igboekwe *et al*. (2006), vertical electrical sounding (VES) is a geophysical technique for determining subsurface geology. It has also been frequently utilized for determining aquifer potential in borehole drillings. Emenike (2001), Onwuemesi & Egboka (2006) and Okoro *et al*. (2010) have also been successful with the vertical electrical approach. (Tizro *et al*., 2010) used VES to determine aquifer depths, transmissivity of rocks and soils, and the geometry of aquifers, geologic formations, and hydro stratigraphic sequences. Raouf & Mesalam (2016) studied the limestone karst system's topsoil of west Iran, while Odoh *et al*. (2012) used an integrated array of geophysical approaches to prospect for groundwater in a fractured shale aquifer of Kpiri-Kpiri, Ebonyi State, Southeast Nigeria. Also, Nejad *et al*. (2011) utilized electrical resistivity method to study subsurface layers and determine aquifer features.

Electrical resistivity tomography is a non-destructive, non-invasive, portable, and environmentally benign technique with a wide range of applications in engineering, environmental science, and subsurface geology (Metwaly, 2012). As stated by Griffiths & Barker (1994), to better understand complicated subsurface formations, electrical resistivity tomography was invented. It is utilized to obtain high-resolution images of subsurface electrical resistivity patterns. It is also used to evaluate how apparent resistivity is distributed horizontally per depth. When used in geological mapping and groundwater investigations, 2-D electrical resistivity tomography has proven to be effective (Zhou *et al*., 2004, Hsu *et al*., 2010 and Rao *et al*., 2013). Even in the presence of geological and topographical difficulties, electrical resistivity tomography (ERT) provides a more accurate 2-D resistivity model of the subsurface, where resistivity variations in the vertical as well as horizontal directions along the survey line are recorded continuously (Loke *et al*., 2013). According to Yang *et al*. (2002), Hauck *et al*. (2003), Cheng *et al*. (2008) and Crook *et al*. (2008), 2D ERT approach is a more effective and powerful way for studying shallow subsurface electrical structures in a variety of situations. Groundwater exploration and prospecting, engineering geophysics and environmental site evaluations have all made substantial use of electrical resistivity tomography (eg., Hossain, 2000; Suzuki *et al*., 2000; Demanet *et al*., 2001; Adepelumi *et al*., 2006; Gokturkler *et al*., 2008; Andrade, 2011). Using 2D electrical resistivity tomography, Alshehri & Abdelrahman (2021) investigated the groundwater supply of the Harrat Khaybar area in Saudi Arabia, determining the water bearing formation to be sub-basaltic alluvial sediments and basaltic flows. Niculescu & Andrei (2021) used electrical resistivity tomography to image sea water intrusion in the coastal aquifer of Romania's Vama Veche resort, showing abnormal zones that were 45–49 m deep and delineating potential salt water intrusion channels in the area. 2D electrical resistivity tomography play a very important role in environmental studies, one typical example is by Ugbor *et al*. (2021) that studied the influence of leachate plumes on groundwater around dumpsites.

LOCATION AND TOPOGRAPHY

The study area is located in Plateau State, Langtang South Local Government Area, in the north-central part of Nigeria. It lies within latitudes N 08° 43′ 45″ and N 08° 44′ 15″ and longitudes E 009° 42′ 15″ and E 009° 43′ 45″ on a scale of 1:10,000. It is extracted from Shendam South-west Sheet 212 with an aerial extent of 25 km^2 (Figure 1).

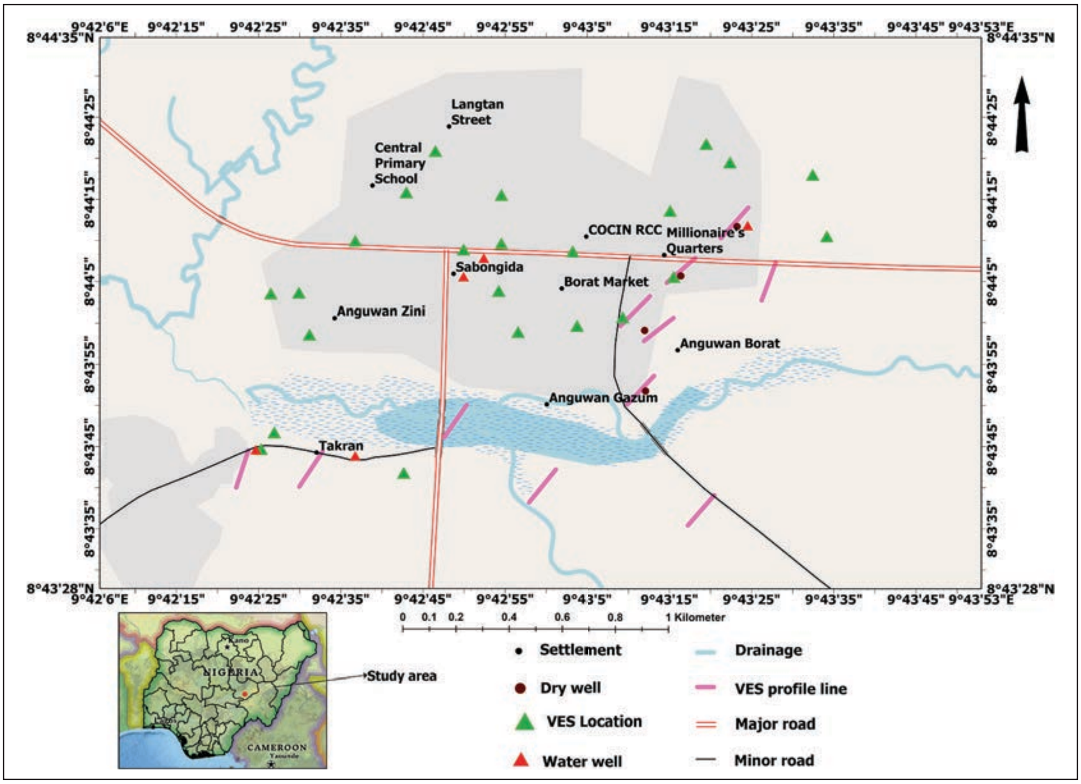

Figure 1: Location Map of Sabongida, North Central Nigeria.

The area is accessible through Yelwa–Shendam–Yelwa–Sabongida and Zamko-Mabudi Trunk 'A' and Trunk 'B' roads with many rural roads and footpaths linking the area to Sabongida. The roads are in a bad shape and this made it difficult to access the community for any groundwater exploration work. There are lots of footpaths and cattle tracks connecting the study area and other open sources of domestic water. The area lacks basic social amenities like electricity, medical care facilities, potable water and road network. The absence or lack of these basic necessities makes life difficult to the general population of the locality.

The relief of the study area is characterised by undulating planes that has been affected by erosion and weathering. The area is composed of lowland with few denudated low laying conical hill with flat tops. Laterization is also observed along most of the river channels which are situated in low elevated areas. The low-lying hills are easily noticed because the hills have been greatly reduced to almost near horizontal plain. The streams and rivers normally dry up during the dry season leaving behind mud cracks and stagnant ponds but they flow during the wet or rainy season when the ground is sufficiently recharged by rainfall. The area experience scarcity of water during the dry season. The water flow majorly from the north to the south during the rainy season. The rivers have many tributaries at various points due to the topography of the area.

GEOLOGY OF THE STUDY AREA

The study area is part of the Central Benue trough which is located between the NE-SW trending rift valley estimated to extends to 1000 km long and about 150 km wide (Obaje, 2004). The area is predominantly underlain by a shale formation (Figure 2). The Awgu Formation in the Central Benue trough plainly indicates the end of marine sedimentation (Offodile, 1976; Ofoegbu, 1990). Sandstones, siltstones and coal beds make up the formation, which includes bluish-grey to dark-black carbonaceous shales, calcareous shales, shale and limestones, sandstones, and siltstones. The major outcrop of the coal-bearing Awgu Formation is mentioned by Obaje (1994) and it does not extend to Sabongida in Langtang South in Plateau State. The Lafia Formation which is the youngest formation in the Central Benue trough does not extend to the Sabongida area, the formation was deposited under continental condition (fluviatile) in the Maastrichtian and lies unconformably on the Awgu Formation. (Obaje, 2004) subdivided the entire Central Benue trough into six stratigraphic units, they are Albian which include the Gboko Formation referred to as the Asu River Group (Offodili, 1976; Nwajide, 1990) which are overlain by Cenomanian Awe and Keana formations. The Cenomanian–Turonian Ezeaku Formation overlies the Keana Formation. The coal rich Agwu Formation which is late Turonian – Early Santonian overlies the Ezeaku Formation and is covered by the Campanon - Maastrichian

Lafia Formation which is the youngest formation (Obaje, 2004). The predominantly Agwu Formation is associated with conglomerate of laterite overlying shale (Plate 1A). The thickness of the conglomerate ranges from 1.5 to 3 m, the conglomerates serve as good materials for road constructions and also serve as overburden aquifer in shallow wells.

The lateritic formation is an unconformity between the Agwu Formation and Lafia Formation. The lateritic conglomerate is the period of the unconformity. The conglomerate deposition resulted during the change in water surge from low to high current. This conglomerate can also serve as water bearing formations, one typical example is the Kerri-Kerri Formation of the Chad basin. Unconformity separates the Agwu Formation from the Lafia Formation and this confirmed the fact that either the Lafia Formation does not extend to the study area or it may have been eroded. The thickness of the conglomerate tends to increase northwards which explains why the communities situated northwards have little water scarcity compared to those situated southward where the conglomerates thin out. Carbonaceous shales, calcareous shales, shaly limestones, sandstones, and siltstones make up the Agwu, the formation found here is the whitish type (Plate 1B), which means they were deposited at the shallow part of the Central Benue trough and therefore susceptible to oxidation.

Sabongari has no visible outcrops and the formation is relatively undeformed because there are no major structures observed during the geologic mapping. The outcrops seen are from the burrows pit excavated by a construction company.

MATERIALS AND METHODS

Vertical electrical sounding (VES)

Ohm mega resistivity meter was used for carrying out the vertical electrical sounding (VES) and ADMT 600S - X equipment for electrical resistivity tomography (ERT). A total of 22 vertical electrical soundings and 11 2D electrical resistivity tomography points were carried out. The use of the electrical resistivity method as a geophysical tool for exploration is based on the movement of electric current through the ground and rock material (Aning *et al.*, 2014). To allow electrical current to travel through the

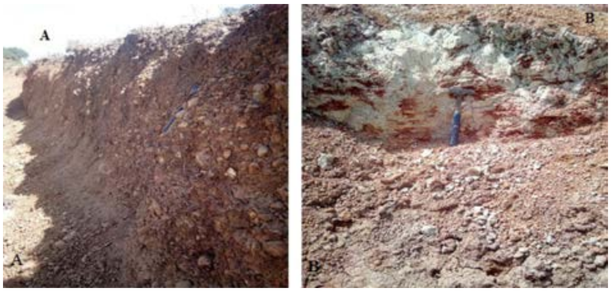

Plate 1: (A) Typical bed of conglomerate (unconformity period) overlaying shale formation, (B) Whitish grey shale deposited in an oxidizing environment.

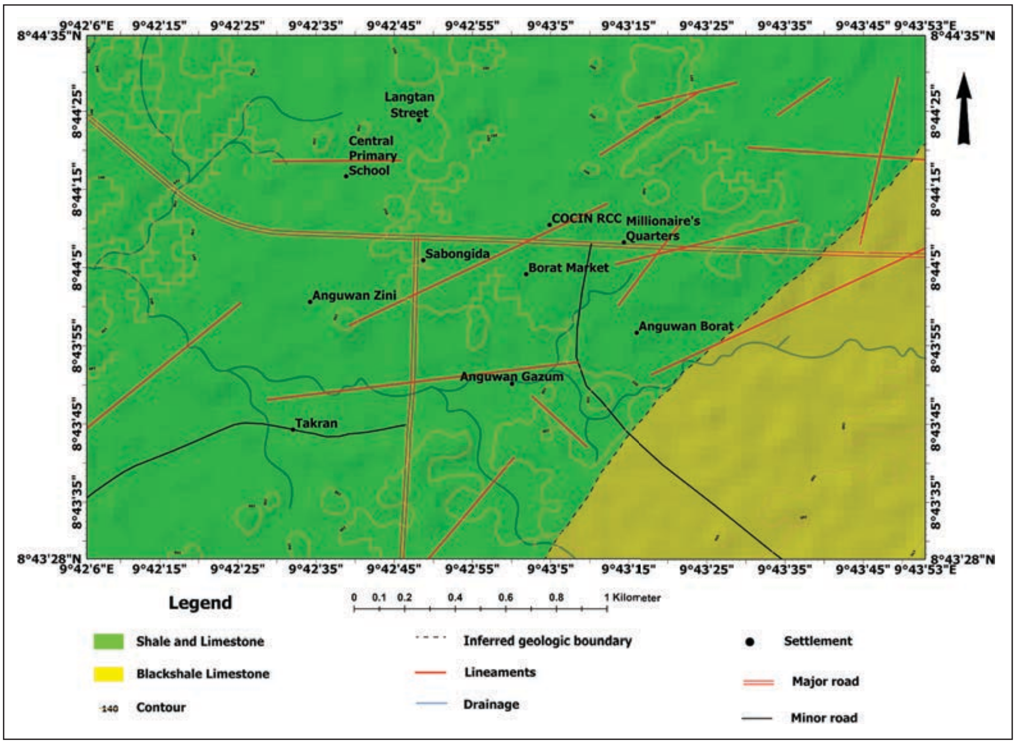

Figure 2: Geological Map of Sabongida.

ground, a rock must have some electrical resistance and the ability to store electrical charges (Aning *et al*., 2014). Vertical electrical sounding (VES) was used to determine the vertical geologic variation of resistivity in the area using a Schlumberger configuration. The relative spacing of the current and potential electrodes is maintained, and the entire spread is gradually increased around a fixed central point. On the earth's surface, four electrodes in the sequence A M N B are set in a straight line, with AB ≥ 5 MN. The apparent resistivity (a) measured with a Schlumberger array, where AM is the distance between the positive current electrode A and the potential electrode M on the earth's surface. When two current electrodes A and B are utilized, the potential difference (V) between two measured electrodes M and N is detected, the apparent resistivity can be written in the form:

$$\rho a = \pi\ \Delta V/I \times [\ ((AB/2)2 - (MN/2)2)\ /\ MN]\ \text{or}$$
$$\rho a = \pi\ K\ \Delta V/I \qquad \text{(Eqn. 1)}$$

The apparent resistivity (ρ) is determined by the electrode array geometry, as defined by the geometric factor (K) (Reynolds, 1997).

2D electric resistivity tomography (ERT)

2D electrical resistivity tomography (ERT) is a technique for imaging the subsurface bulk electrical resistivity distribution. It enables the mapping of the Earth's electrical resistivity distribution, allowing for subsurface heterogeneity estimation (Slob, 2004). When current is injected into the ground using two current electrodes, the ground surface (layers of materials with different individual resistivity) may be measured, allowing the subsurface resistivity distribution to be determined (Herman, 2001; Loke *et al*., 2013). The critical part in ERT is computing the resistivity pseudo section (Everett, 2013). The observed apparent resistivity is used to match the pseudo section in ERT imaging. The ERT measurement can be converted into high-resolution resistivity images in 1-D, 2-D, and 3-D. ERT is regarded better than other electrical approaches since quantitative findings are obtained by using a regulated source of specific dimensions (Telford *et al*., 1990). Geological characteristics such as mineral, fluid content, porosity and degree of water saturation also have a significant impact on electrical properties (Loke *et al*., 2013; Aizebeokhai *et al*., 2015). The potential difference is converted into resistivity of the subsurface strata (Reynolds, 1997). 2D methodologies of electrical resistivity tomography was discussed in detailed by (Gharibi & Bentley, 2005; Chambers *et al*., 2007, 2011; Magnusson, *et al*., 2010). For the purpose of this study, the instrument ADMT 600 S - X is used for ERT. It is a geophysical instrument comprising of two electrodes, connecting cables and a main frame with touch screen or a sensor probe which could be used in place of the electrode. A measuring tape is used to measure the distance of the spread on the ground. The principles of the instrument is based on electrical resistivity method which is measured through the potential electrode and the result presented as 2D images (electrical resistivity tomography) with various color to represent different formation as the resistivity changes.

RESULTS

Vertical electrical sounding (VES)

In this study, 22 vertical electrical sounding (VES) measurements were taken. The resistivity values, layer thickness, and depth of the VES survey data collected from various places within the research region were analyzed and the results presented in Figures 3, 4, 5 and 6. 9.1 % of the curves in Sabongida are Q type and 40.9 % are HK curves while the dominant field curves in the study area are H type curve making up to 50 % of the curves. Qualitative interpretation of electrical soundings revealed a general view on the lateral and vertical variations in the apparent resistivity and geology of the study area.

The results of interpreted curves are presented in Table 1. In terms of electrical resistivity, igneous and metamorphic rocks have higher resistivity values compared to most sedimentary rocks such as shale and sandstones. The resistivity values of the first layer ranges from 70 to 750 Ωm and the thickness ranging from 1.6 to 6 m, this indicates that the layer consists of a lateritic cap. The second layer with apparent resistivity value ranging from 15 to 220 Ωm and a range of thickness from 3 to 33 m, this layer is of clayey sand and shale formations. The third layer on the other hand ranges from 1 to 65 Ωm and the thickness ranges from 10.5 to 160 m.

2D electrical resistivity tomography (ERT)

Eleven (11) profile lines were conducted, each covering a horizontal length of 20 m with a probing depth of 300 m, except for profile number 11 that has a depth of 400 m. The distance between the probes (sensors) is 2 m and the result is presented as a 2D image which is known as electrical resistivity tomography with each color representing the range of resistivity values in ohms - meter (Ωm). The results of all the 11 profiles conducted within the study area are presented as electrical resistivity tomography, the Y axis is representing the depth while the X - axis represents distance on the ground. The blue color represents range of resistivity values which are conductive in nature with low resistivity values (water saturated, shale or loose sediment) while light green to red color represent geologic materials that are average to high resistive materials or consolidated in nature. In most cases the low resistivity is attributed to factors such as the porosity, permeability, water content, temperature and clay in the soil. Figure 7(P1) shows green color indicating sandy formation from 0 to 170 m with pockets of high

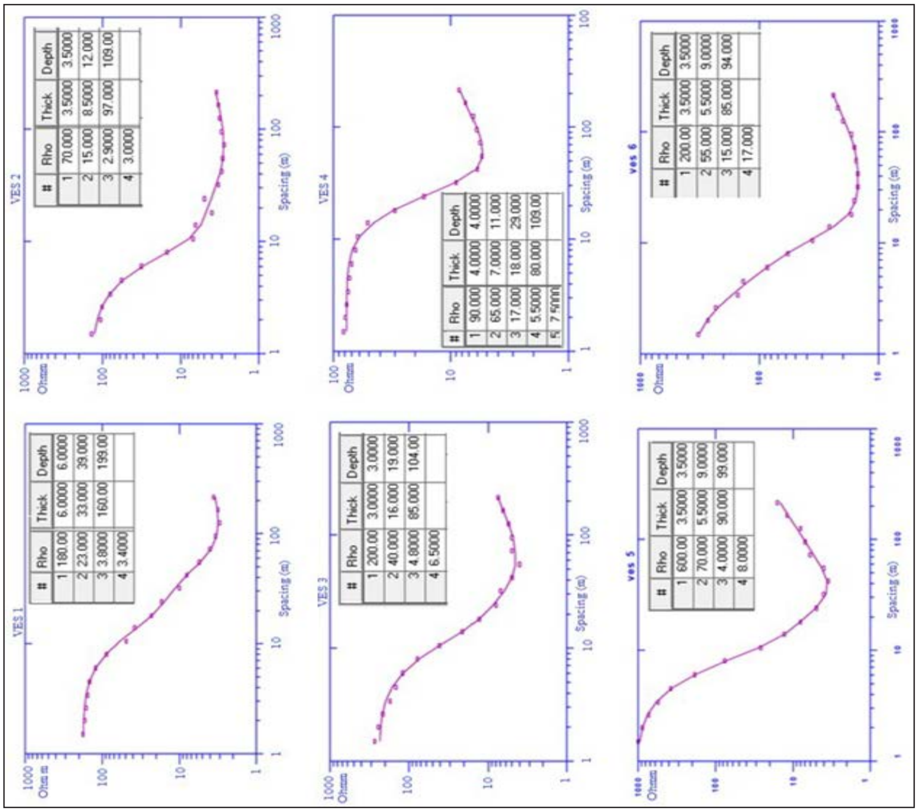

Figure 3: Vertical electrical sounding curves of VES 1 - 6.

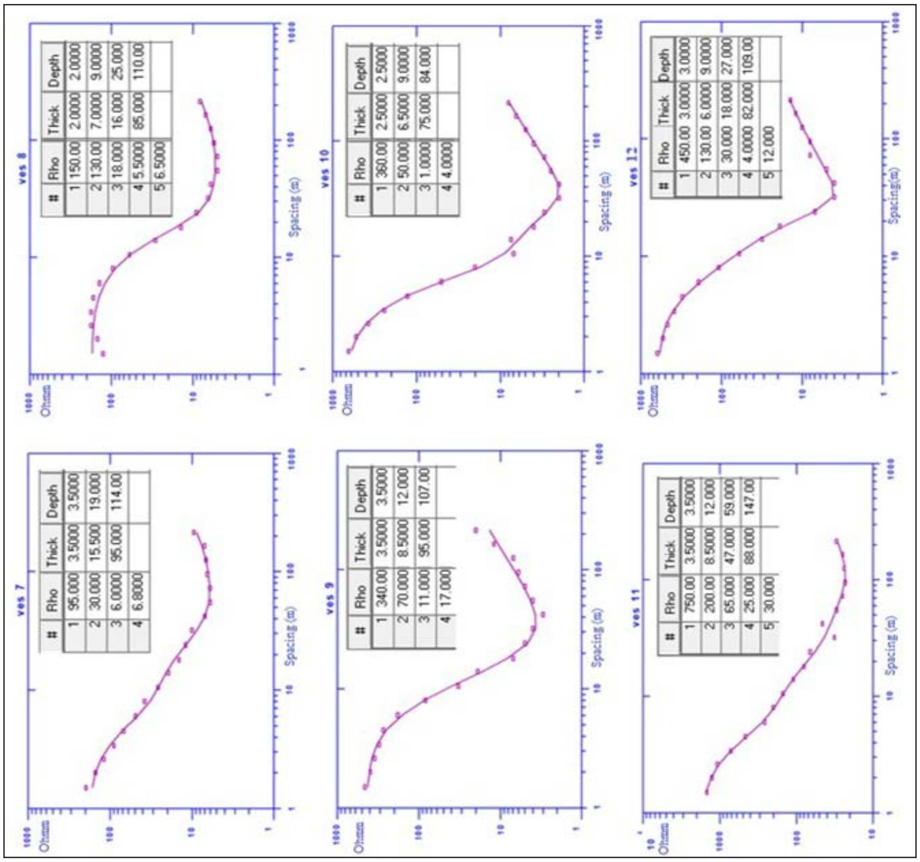

Figure 4: Vertical electrical sounding curves of VES 7 - 12.

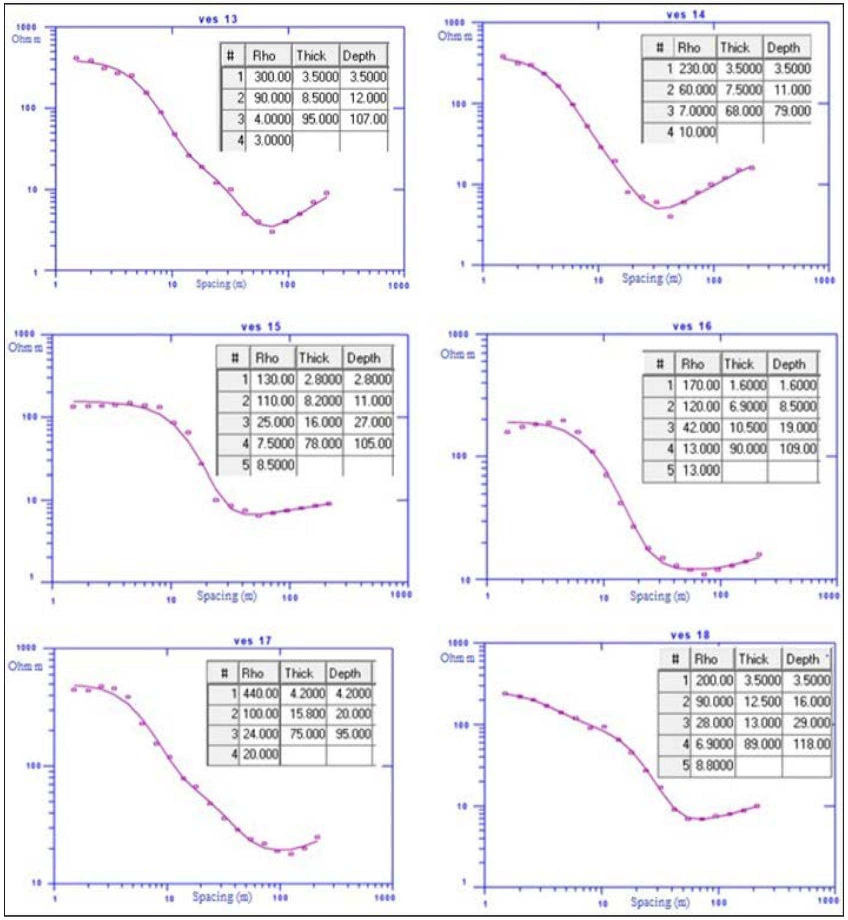

Figure 5: Vertical electrical sounding curves of VES 13 - 18.

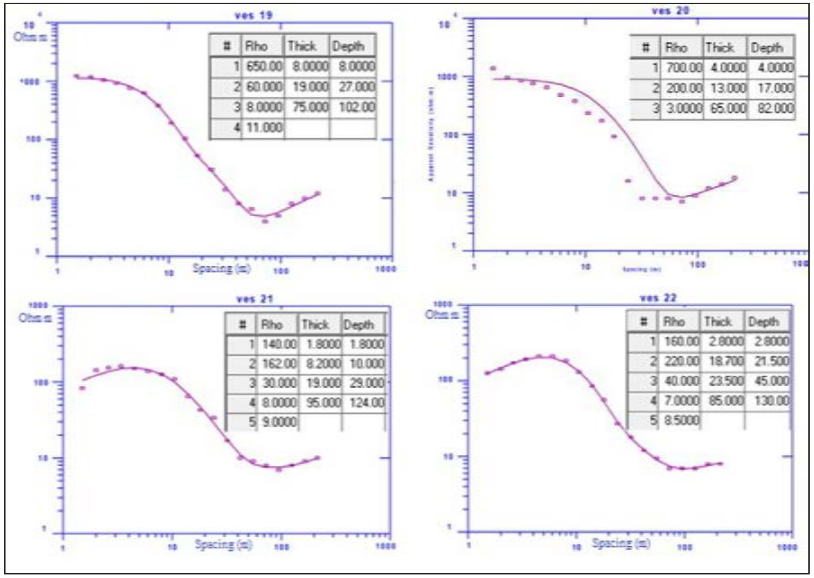

Figure 6: Vertical electrical sounding curves of VES 19 – 22.

Table 1: Vertical electrical sounding locations, coordinates and geoelectric parameters.

S/No	Location	Coordinate		Resistivity (Ωm)					Thickness (m)			
		Lat.	Long.	1	2	3	4	5	1	2	3	4
1	VES 1	08° 44' 10.8"	009° 42' 54.3"	180	23	3.8	3.4		6	33	160	
2	VES 2	08° 44' 16.5"	009° 42' 54.3"	70	15	2.9	3		3.5	8.5	97	
3	VES 3	08° 44' 09.5"	009° 42' 5.0 "	200	40	4.8	6.5		3	16	85	
4	VES 4	08° 44' 16.3"	009° 42' 43.1"	90	65	17	5.5	7.5	4	7	18	80
5	VES 5	08° 44' 21.3"	009° 42' 46.5"	600	70	4	8		3.5	5.5	90	
6	VES 6	08° 44' 10.9"	009° 42' 37.0"	200	55	15	17		3.5	5.5	85	
7	VES 7	08° 44' 04.2"	009° 42' 30.1"	95	30	6	6		3.5	15.5	95	
8	VES 8	08° 43' 59.2"	009° 42' 31.4"	150	130	18	5.5	6.5	2	7	16	85
9	VES 9	08° 43' 45.0"	009° 42' 25.6"	340	70	11	17		3.5	8.5	95	
10	VES 10	08° 43' 42.8"	009° 42' 42.7"	360	50	1	4		2.5	6.5	75	
11	VES 11	08° 43' 21.3"	009° 42' 37.9"	750	200	65	25	30	3.5	8.5	47	88
12	VES 12	08° 44' 04.8"	009° 42' 54.2"	450	130	30	4	12	3	6	18	82
13	VES 13	08° 43' 59.5"	009° 42' 56.5"	300	90	4	3		3.5	8.5	95	
14	VES 14	08° 44' 00.4"	009° 43' 03.9"	230	60	7	10		3.5	7.5	68	
15	VES 15	08° 44' 01.6"	009° 43' 09.1"	130	110	25	7.5	8.5	2.8	8.2	16	78
16	VES 16	08° 44' 06.3"	009° 43' 15.3"	170	120	42	13	13	1.6	6.9	10.5	90
17	VES 17	08° 44' 14.4"	009° 43' 14.9"	440	100	24	20		4.2	15.8	75	
18	VES 18	08° 44' 09.6"	009° 43' 03.2"	200	90	28	6.9	8.8	3.5	12.5	13	89
19	VES 19	08° 44' 11.0"	009° 43' 33.8"	650	60	8	11		8	19	75	
20	VES 20	08° 44' 18.5"	009° 43' 32.2"	700	200	3			4	13	65	
21	VES 21	08° 44' 13.3"	009° 43' 23.9"	140	162	30	8	9	1.8	8.2	19	95
22	VES 22	08° 44' 20.3"	009° 43' 22.2 "	160	220	40	7	8.5	2.8	18.7	23.5	85

resistive lateritic sand on top and toward the end of the profile with resistivity values ranging from 215 to 315 Ωm and, a thin layer of laterite intercalated with shale of 30 m thick. Figure7(P2) revealed thick layer of shale of 100 m which is overlain by sand/lateritic material and a thin resistive horizontal lateritic material on point 20. Figure 7(P3) present thin layers of shale/sand formation at different depth levels with resistivity values ranging from 115 to 220 Ωm. Deposits of sand/lateritic materials with resistivity values of 255 to 360 Ωm at 150 m. The over burden materials are predominant lateritic with resistivity values of 360 to 465 Ωm with thickness of 60 m.

The electrical resistivity tomography in Figure 8(P4, P5 and P6) are characterized by thick overburden lateritic materials of 90 m and resistivity values ranging from 160 to 345 Ωm. Thin layers of shales were observed in P4 at 150 and 180 to 230 m depths and a wide layer of sandy/lateritic materials were revealed at 240 to 300 m with resistivity values ranging from 100 to 265 Ωm.

The electrical resistivity tomography in Figure 9 reveal laterite at the top of profile P7, and underlain by a layer of sand with resistivity values ranging from 145 to 215 Ωm. Thin layer of intercalation of shale/sand were delineated at 150 to 300 m. Figure 9(P8) shows a thick layer of sand of 0 to 140 m which is separated by a thin layer of resistive lateritic material. A thin layer of shale/sand formation of 70 m thick with resistivity values of 115 to 175 Ωm were recorded. Figure 9(P9) presents a resistive lateritic/sand formation of 120 m thick which is underlain by lateral layer of shale/sand of 30 m at 180 m and 270 m.

The electrical resistivity tomography in Figure 10 (P10) revealed a thick layer of sand as the overburden formation in the area with resistivity values of 135 to 180 Ωm, and thin resistive horizontal materials suggesting lateritic materials. Thin layer of shale/sand is interbedded within lateritic materials at 260 m with resistivity values ranging from 180 to 240 Ωm. The electrical resistivity tomography in Figure10(P11) are characterized by thick shale/sandy formation of 160 to 180 m, 240 to 300 m, 320 to 340 m and 355 to 370 m with their resistivity values ranging from 70 to 150 Ωm.

DISCUSSION

The geology of the study area is predominantly underlain by late Cretaceous Agwu Formation. The Agwu Formation was deposited in a marine environment and are structurally controlled in the NE–SW direction, and

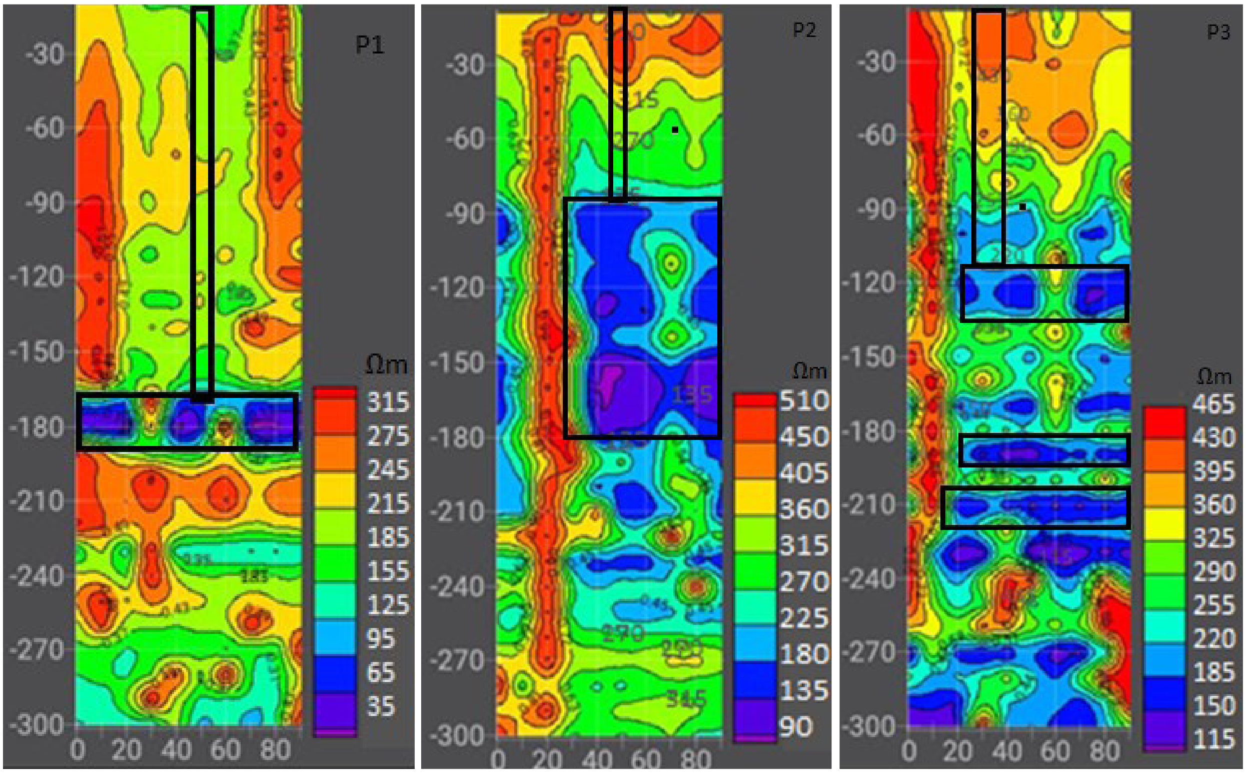

Figure 7: Electrical resistivity tomography of profile P1, P2 and P3.

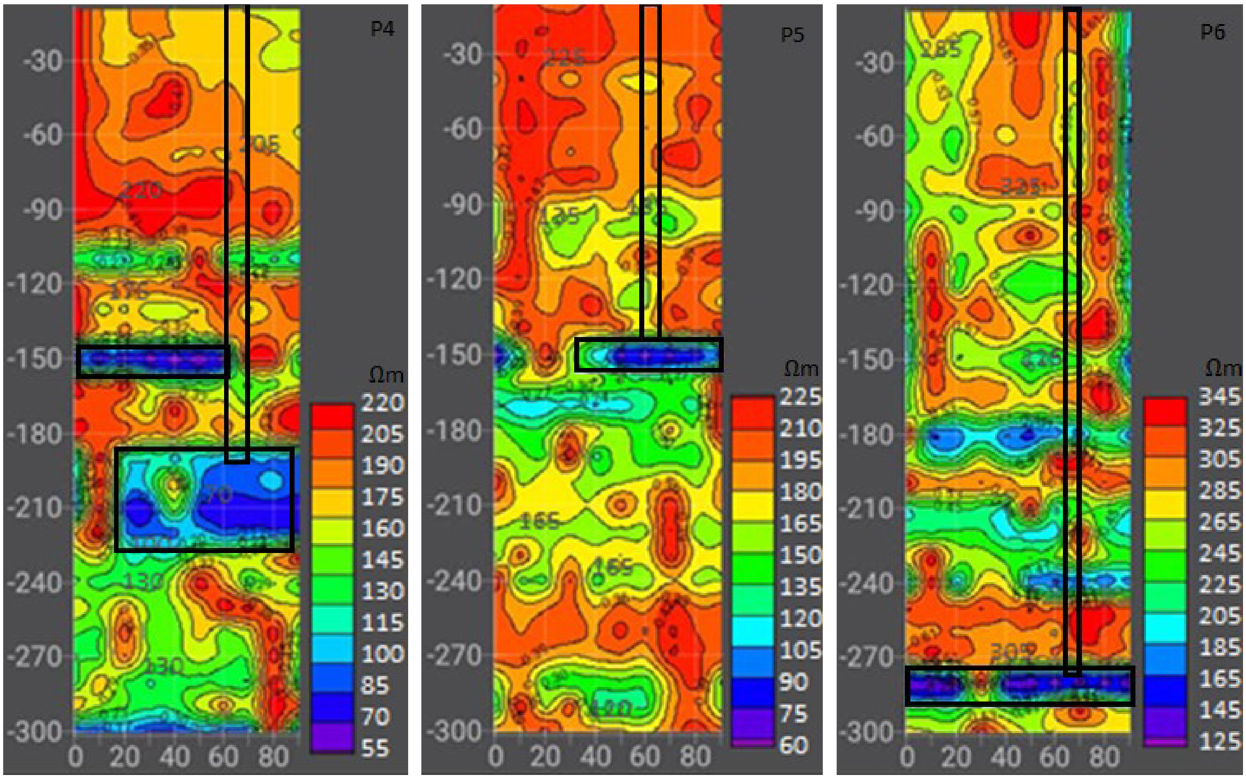

Figure 8: Electrical resistivity tomography of profile P4, P5 and P6.

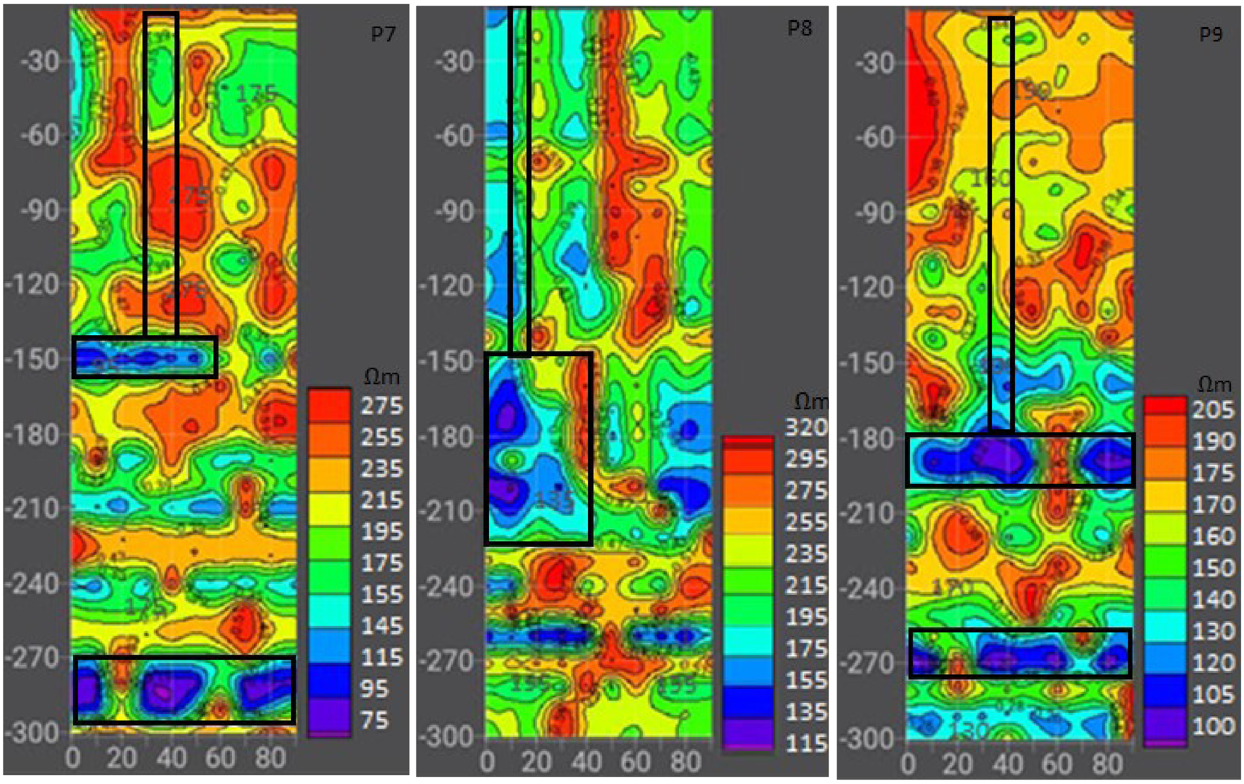

Figure 9: Electrical resistivity tomography of profile P7, P8 and P9.

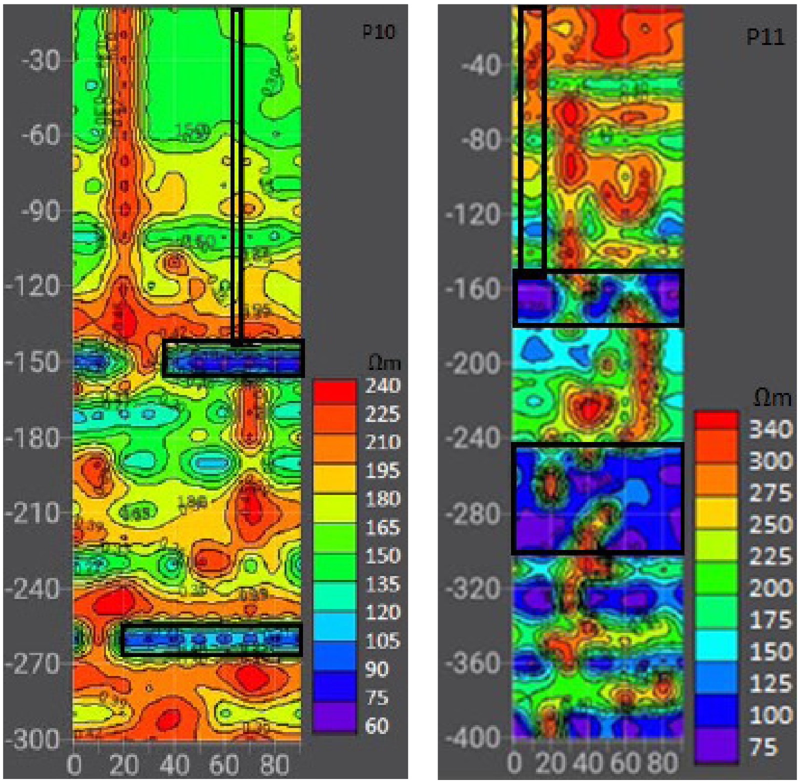

Figure 10: Electrical resistivity tomography of profile P10 and P11.

consists mainly of shale, shelly limestone, sandstone and siltstone (Agumanu, 2011). At some locations, the Agwu Formation is overlain by Agbani Formation which is sandstone in nature with an exposed thickness of 45 m. The shelly nature of the area is responsible for the difficulty in locating optimal drilling points for groundwater exploration in Sabongida. Most of the hand dug wells within the area are shallow and dry up during dry season, creating water scarcity in the community. There are no functional and productive boreholes in Sabogida because all the failed wells were drilled at a very shallow depth, thereby not reaching the potential aquifer (water bearing formation) in the area. The analysis of the results from the geophysical survey identified three different lithologies. The lithologies encountered from the surface to the depth are various lateritic formations (lateritic sand, laterites) with high resistivity values of > 500 Ωm; a shale layer with low resistivity values of < 40 Ωm, and the third layer is of silt stone/shale formation which are the zones of low to moderate resistivity ranging from 50 to 185 Ωm and these are the saturated zones or productive groundwater zones otherwise known as the aquifer in the area.

The electrical resistivity tomography (ERT) over Sabongida revealed deeper lithologic information compared to the vertical electrical sounding due to the electrode spread of AB/2 = 215 m used in this study. The ERT probed 300 m depth with better, clearer and easy to interpret 2D images in terms of the different geologic information in Sabongida. Low resistivity values observed in Figure 7(P1) at the depth of 160 to 200 m suggest saturated layer of sandstone which is a good drilling point for a productive borehole. Figure 7(P2) is characterized by thick shelly layer from 90 to 180 m with resistivity values ranging from 90 to 225 Ωm, this location if carefully screened will yield adequate groundwater to the community and end water scarcity. Figure 7(P3) revealed different layers of shale/sandstone/siltstone with resistivity values of 115 to 325 Ωm, this is in agreement with the local geology of Sabongida (Agumanu, 2011) which is characterized by thick sediments of Agwu Formation. Figure 8(P4, P5, P6) revealed high resistive conglomerate of laterite which are reddish in color. A thin lateral layer of shale/sandstone/siltstone with low resistivity values varying from 55 to 225 Ωm with the thickness of 15 to 35 m were detected, thus these profiles may not be suitable for drilling productive boreholes in the area, with the deepest layer occurring at 270 to 290 m.

Thin layer of low resistivity materials of shales/ siltstone/sand at 150 and 270 to 300 m, possible drilling site is recommended at point 4 (Figure 9(P7)) and should be drilled to the depth of 300 m, the borehole will tap water from different layers of sandstone/siltstone at 150, 210, 240 and 270 to 300 m. P8 in Figure 9 shows large area dominated by green color indicating the presence of low to medium resistivity rocks which is influenced by porosity, clay or water contents. Productive boreholes are recommended at 180 to 210 and 270 to 300 m depths of profile P9 of Figure 9. Thick layer of low to medium resistivity was observed in Figure10(P10) and a thin lateral layer of shale/sandstone/ siltstone at 150 and 260 m, while thick layer of shale/sandstone were revealed at different depth levels in Figure 10(P11), suggesting possible productive site for drilling a borehole for the community.

CONCLUSION

The Sabongida community depends largely on surface water than groundwater sources due to previous abortive boreholes drilled as a result of the complex nature of the geology. This is because the water bearing formation is underlain by a thick shale bed in the area. The results of vertical electrical sounding and 2D electrical resistivity tomography have proved their credibility beyond reasonable doubt to locate possible drilling site in the community. Water scarcity in Sabongida would be a thing of the past if strict compliance to the results and recommendations are followed. It is concluded that there is a good prospect of groundwater if the aquifer is properly located and the screen properly placed during drilling. Groundwater bearing formations are delineated and drilling is recommended to the depth of 150 to 300 m in the area.

ACKNOWLEDGEMENTS

The authors appreciate University of Jos, Nigeria for giving us ADMT 600 X-S and Ohm mega resistivity meter to use for this research work. We are also grateful to the two anonymous reviewers for their helpful comments.

AUTHOR CONTRIBUTIONS

SNY designed the concept of the research and planned the field work. HCD and CMA carried out the field work. The three authors processed and interpreted the data and put it together as a research paper.

CONFLICT OF INTEREST

The authors declare that we have no conflict of interest in this paper.

REFERENCES

Adepelumi, A.A., Yi, M.J., Kim, J.H., Ako, B.D. & Son, J.S., 2006. Integration of surface geophysical methods for fracture detection in crystalline bedrocks of southwestern Nigeria. Hydrogeology Journal, 14, 1284–1306.

Agumanu, A.E., 2011. Environment of deposition of deposition of the Agwu Formation (Late Cretaceous), Southern Benue Trough, Nigeria. Global Journal of Geological Sciences, 9 (2), 215 – 228.

Aizebeokhai, A.P., Oyeyemi, K.D. & Kayode, O.T., 2015. Multiple-gradient array for near-surface electrical resistivity tomography. In Near-Surface Asia Pacific

Conference, Waikoloa Hawaii, 2015. Society of Exploration Geophysicists, Australian Society of Exploration.

Alshehri, F. & Abdelrahman, K., 2021. Groundwater resources exploration of Harrat Khaybar arean northwest Saudi Arabia, Using electrical resistivity tomography. Journal of King Saud University – Science, 33, 2- 7.

Amaresh, K.S., Raviprakash, S., Mishra, D. & Singh, S., 2006. Groundwater potential modeling in Chandraprabha subwater shed, using remote sensing, geoelectrical and GIS.www.gisdevelopment.net.

Andrade, R., 2011. Intervention of electrical resistance tomography (ERT) in resolving hydrological problems of a semiarid granite terrain of southern India. Journal of Geological Society of India, 78(4), 337–344.

Aning, A.A., Sackey, N., Jakalia, I.S., Sedoawu, O., Tetteh, E.H., Hinson, G., Akorlie, R.K., Appiah, D. & Quaye, E.K., 2014. Electrical resistivity as a geophysical mapping tool; A case study of the New Art Department, Knust- Ghana. International Journal of Scientific and Research Publications, 4(1), 1 – 7.

Araffa, S.A.S., 2012. Groundwater management by using hydro-geophysical investigation: Case study: An area located at North Abu Zabal City. National Research Institute of Astronomy and Geophysics, Helwan, Cairo, Egypt, 181 - 202.

Chambers, J.E., Wilkinson, P.B., Kuras, O., Ford, J.R., Gunn, D.A., Meldrum, P.I., Pennington, C.V.L., Weller, A.L., Hobbs, P.R.N. & Ogilvy, R.D., 2011. Three-dimensional geophysical anatomy of an active landslide in Lias Group mudrocks, Cleveland basin, UK. Geomorphology, 125, 472 – 484.

Chambers, J.E., Wilkinson, P.B., Weller, A.L., Meldrum, P.I., Gilvy, R.D. & Caunt, S., 2007. Mineshaft imaging using surface and cross - hole 3D electrical resistivity tomography: A case history from the East Pennine Coalfield, UK. Journal of Applied Geophysics, 62, 324 – 337.

Cheng, P.H., Ger, Y.I. & Lee, S.L., 2008. An electrical resistivity study of the Chelungpu fault the Taichung area, Taiwan. Terr. Atmos. Ocean. Sci., 19, 241-255.

Christopher, O., 2006. Water resources, environment and sustainable development in Nigeria. Journal of Human Ecology, 19(3), 169-181.

Crook, N., Binley, A., Knight, R., Robinson, D.A., Zarnetske, J. & Haggert, R., 2008. Electrical resistivity imaging of the architecture of substream sediments. Water Resour. Res., 44, W00D13. doi:10.1029/2008WR006968.

Demanet, D., Pirard, E., Renardy, F. & Jongmans, D., 2001. Application and processing of geophysical images for mapping faults. Comput. Geosci., 27, 1031– 1037.

Eke, K.T. & Igboekwe, M.U., 2011. Geoelectrical investigation of groundwater in some villages in Ohafia Locality, Abia State, Nigeria. British Journal of Applied Science & Technology, 1(4), 190-203.

Ekwe, A.C., Onu, N. & Onuoha, N., 2006. Estimation of aquifer hydraulic characteristics from electrical sounding data: The case of Middle Imo River basin aquifers, Southern Nigeria. Journal of Spatial Hydrology, 6(2), 121-132.

Emenike, E.A., 2001. Geophysical exploration for groundwater in a sedimentary environment: a case study from Nanka over Nanka Formation in Anambra Basin, southeastern Nigeria. Global Journal of Pure and Applied Sciences, 1, 97-102.

Everett, M.E., 2013. Near-surface applied geophysics. Cambridge University Press. 403 p.

Gharibi, M. & Bentley, L.R., 2005. Resolution of 3-D electrical resistivity images from inversions of 2-D orthogonal lines. Journal of Environmental and Engineering Geophysics, 10, 339 – 349.

Gokturkler, G., Balkaya, C., Erhan, Z. & Yurdakul, A., 2008. Investigation of a shallow alluvial aquifer using geoelectrical methods: A case from Turkey. Environ. Geol., 54, 1283–1290.

Griffiths, D. & Barker, R., 1994. Electrical imaging in archaeology. Journal of Archaeological Science, 21(2), 153-158.

Gyau-Boakye, P., Kankam-Yeboah, K., Dapaah-Siakwan, S. & Darko, P. K., 2008. Groundwater as vital resource for rural development: An example from Ghana. In: A.M. Segun Adelana, (Ed.), Applied groundwater studies in Africa. Taylor & Francis, London, 149-170.

Hauck, C., Muhll, D.V. & Maurer, H., 2003. Using DC resistivity tomography to detect and characterize mountain permafrost. Geophysical Prospecting, 51, 273-284.

Herman, R., 2001. An introduction to electrical resistivity in geophysics. American Journal of Physics, 69(9), 943-952.

Hewaidy, A.A., El-Motaal, E.A., Sultan, S.A., Ramdan, T.M., El khafif, A.A. & Soliman, S.A., 2015. Groundwater exploration using resistivity and magnetic data at the northwestern part of the Gulf of Suez, Egypt. Egyptian Journal of Petroleum, 24(3), 255-263.

Hossain, D., 2000. 2D electrical imaging survey in hydrogeology. The Bangladesh J. Sediment. Res., 18(1), 57–66.

Hsu, H., Yanites, B.J., Chih, C. & Chen, Y., 2010. Bedrock detection using 2D electrical resistivity imaging along the Peikang river, central Taiwan. Geomophology, 114, 406 – 414.

Igboekwe, M.U., 2005. Geoelectrical exploration for groundwater potentials in Abia State, Nigeria. Unpublished Ph.D Thesis. Michael Opara University of Agriculture, Umidike, Nigeria.

Igboekwe, M.U., Okwueze, E.E. & Okereke, C.S., 2006. Delineation of potential aquifer zones from geoelectric soundings in Akwa Ibom River watershed, Southwestern Nigeria. Journal of Engineering and Applied Science, 1(4), 410 – 421.

Loke, M.H., Chambers, J.E., Rucker, D.F., Kuras, O. & Wilkinson, P.B., 2013. Recent developments in the direct-current geoelectrical imaging method. Journal of Applied Geophysics, 95, 135-156.

Magnusson, M.K., Fernlund, J.M.R. & Dahlin, T., 2010. Geoelectrical imaging in the interpretation of geological conditions affecting quarry operations. Bulletin of Engineering Geology and the Environment, 69, 465 – 486.

Metwaly, M., 2012. Groundwater exploration using geoelectrical resistivity technique at AlQuwy'yia area Central Saudi Arabia. International Journal of the Physical Sciences, 7(2), 317 – 326.

Nejad, H.T., Mumipour, M., Kaboli, R. & Najib, O.A., 2011. Vertical electrical sounding (VES) resistivity survey technique to explore groundwater in an arid region. Journal of Applied Sciences, 11(23), 3765 - 3774.

Niculescu, B.M. & Andrei, G., 2021. Application of electrical resistivity tomography for imaging seawater intrusion in a coastal aquifer. Acta Geophysica, 69, 613 – 630.

Nwajide, C.S., 1990. Createaceous sedimentation and palaeogeography of the Central Benue Trough. In: C. O. Ofoegbu, (Ed.), The Benue Trough, structure and evolution.

International Monograph Series, Friedrich Vieweg Und Sohn, Braunschweig, 19 – 38.
Obaje, N.G., 1994. Coal petrography, microfossils and paleoenvironments of Cretaceous coal measures in the middle Benue Trough of Nigeria. Tubinger Mikropalaontlogische Mittei lungen, 11, 1-150.
Obaje, N.G., 2004. Geology and mineral resources of Nigeria. Springer, Dordrecht Heidelbug London New York. 222 p.
Obiadi, I.I., Obiadi, C.M., Akudinobi, B.E.B., Maduewesi, U.V. & Ezim, E.O., 2016. Effects of coal mining on the water resources in the communities hosting the Iva valley and Okpara coal mines in Enugu state, south east Nigeria. Sustain. Water Resour. Manag., 2(3), 207 - 216.
Offodile, M. E., 1976. The geology of the Middle Benue Trough, Nigeria. Publication from the Palaeontological Institution of the University of Uppsala, 4, 1- 167.
Ofoegbu, C.O., 1990. Benue Trough structure and evolution. International Monograph Series, Friedrich Vieweg Und Sohn, Braunschweig. 386 p.
Ojo, J.S., Olorunfemi, M.O. & Omosuyi, G.O., 2007. Geoelectric sounding to delineate shallow aquifers in the coastal plain sands of Okitipupa area, southwestern Nigeria. Online Journal of Earth Science, 4, 170-179.
Okoro, E.I., Egboka, B.C.E., Anike, O.L. & Enekwechi, E.K., 2010. Evaluation of groundwater potentials in parts of the escarpment area of South Eastern Nigeria. International Journal of Geomatics and Geosciences, 1(3), 544 – 551.
Onimisi, M., Daniel, A. & Kolawole, M.S., 2013. Vertical electrical sounding investigation for delineation of geoelectric layers and evaluation of groundwater potential in Ajagba, Asa and Ikonofin localities of Ola Oluwa local government area of Osun State, South Western Nigeria. Research Journal of Applied Sciences, Engineering and Technology, 6(18), 3324-3331.
Onwuemesi, A.G. & Egboka, B.C.E., 2006. 2-D polynomial curve fitting techniques on water table, and hydraulic gradients estimations in parts of Anambra Basin, southeastern Nigeria. Natural and Applied Sci. J., 7(1&2), 6 -13.
Rao, B. V., Prasad, Y. S. & Reddy, K.S., 2013. Hydrogeophysical investigations in a typical Khondalitic terrain to delineate the kaolinised layer using resistivity imaging. Journal Geological Society of India, 81, 521-530.
Raouf, A. & Mesalam, M., 2016. Implementation of magnetic, gravity and resistivity data in identifying groundwater occurrences in El Qaa Plain area, Southern Sinai, Egypt. Journal of Asian Earth Sciences, 128, 1 - 26.
Reynolds, J.M., 1997. An introduction to applied and environmental geophysics. John Wiley and Sons Ltd., Chichester, England. 796 p.
Rosen, S. & Vincent, J., 2014. Household water resources and rural productivity in sub-saharan Africa: A review of the Evidence. Harvard Institute for international development Cambridge, MA. 52 p.
Slob, E., 2004. Optimal acquisition and synthetic electrode arrays. SEG Technical Program Expanded, Society of Exploration Geophysicists, 1389 – 1392.
Soupios, P.M., Kouli, M., Vallianatos, F., Vafidis, A. & Stavroulakis, G., 2005. Estimation of aquifer parameters from surficial geophysical methods. A case study of Keritis Basin in Crete. Journal Hydrology, 338, 122 - 131.
Suzuki, K., Toda, S., Kusunoky, K., Fujimitsu, Y., Mogi, T. & Jomori, A., 2000. Case studies of electrical and electromagnetic methods applied to mapping active faults beneath the tick Quaternary. Eng. Geol., 56, 29–45.
Telford, W.M., Geldart, L.P. & Sheriff, R.E., 1990. Applied geophysics. Vol. 1. Cambridge University Press, Cambridge. 760 p.
Thapa, R., Ravindra, K. & Sood, R.K., 2008. Study of morphotectonics and hydrogeology for groundwater prospecting using remote sensing and GIS in the North West Himalaya, District Sirmour, Himachal Pradesh India. International Archives of the Photogrammetry, Remote Sensing and Spatial Information Sciences, 37 (B4), 227-232.
Tizro, A.T., Voudouris, K.S., Salehzade, M. & Mashayekhi, H., 2010. Hydrogeological framework and estimation of aquifer hydraulic parameters using geoelectrical data: A case study from West Iran. Hydrogeology Journal, 18, 917-929.
Ugbor, C.C., Ikwuagwu, I.E. & Ogboke,O.J., 2021. 2D inversion of electrical resistivity investigation of contaminant plume around a dumpsite near Onitsha express way in southeastern Nigeria. Scientific Report, 11(1), 1-14.
Yang, C.H., Chang, P.H., You, J.I. & Tsai, L.L., 2002. Significant resistivity changes in the fault zone associated with the 1999 Chi-Chi earthquake, West Central Taiwan. Tectonophysics, 350, 299-313.
Zhou, Q. Y., Matsui, H. & Shimada, J., 2004. Characterization of the unsaturated zone around a cavity in fractured rocks using electrical resistivity tomography, J. Hydraulic Res., 42, 25 – 31.

Manuscript received 30 September 2021;
Received in revised form 25 January 2022;
Accepted 28 January 2022
Available online 26 April 2022

DOI : https://doi.org/10.7186/wg481202203

Application of Schmidt hammer rebound test for weathering profile classification of granite, Paya Terubong, Penang, Malaysia

Mohamad Anuri Ghazali[1,*], Mohd Rozi Umor[2], Mohd Syafiq Hussin[3], Abdul Ghani Md. Rafek[4]

[1,3,4] Geo Mag Engineering, Tingkat 2, Jalan Pelabur B, 23/B, Seksyen 23, 40300 Shah Alam, Selangor, Malaysia
[1,2] Program Geologi, Pusat Pengajian Sains Sekitaran dan Sumber Alam Fakulti Sains dan Teknologi, Universiti Kebangsaan Malaysia, 43600 Bangi, Selangor D.E., Malaysia
* Corresponding author email address: mohamadanuri16@gmail.com

Abstract: Weathering profile characterization is one of the significant information in the interpretation of the condition of rock. In addition, the tropical climate in Malaysia causes the deep–seated weathering phenomena of granitic rock. The identification of weathering profile of granite can be made using in–situ Schmidt hammer rebound test which is one of the non–destructive tests (NDT) that is widely used. In this study, the test is carried out on granitic rock in Paya Terubong, Pulau Pinang. Based on the study conducted, the value for each of weathering grade of granite can be identified. The value for fresh granite (Grade I) is greater than 55, slightly weathered granite (Grade II) is ranging from 35 – 55, moderately weathered granite (Grade III) is ranging from 17 – 35 and highly weathered granite (Grade IV) is less than 17. Completely weathered granite (Grade V) and residual soil (Grade VI) do not have any Schmidt hammer rebound values. This method can be used as a very useful method in the field to determine the degree of weathering of rock outcrops.

Keywords: Granite, weathering grade, weathering profile, Schmidt hammer rebound test

Abstrak: Pencirian luluhawa adalah salah satu informasi penting dalam menafsir keadaan suatu singkapan batuan. Malaysia yang mempunyai iklim tropika yang telah menyebabkan fenomena luluhawa yang tebal dan dalam bagi batuan granit. Pengenalpastian profil luluhawa granit boleh dilakukan dengan menggunakan kaedah ujian lantunan tukul Schmidt in-situ yang merupakan salah satu kaedah ujian tanpa musnah (NDT) yang sering digunakan. Dalam kajian ini, ujian lantunan tukul Schmidt dijalankan ke atas batuan granit di Paya Terubong, Pulau Pinang. Berdasarkan kajian yang telah dijalankan, nilai lantunan tukul Schmidt bagi setiap gred luluhawa batuan granit dapat dikenalpasti. Nilai bagi batuan granit segar (Gred I) adalah melebihi 55, bagi batuan granit sedikit terluluhawa (Gred II) adalah dalam lingkungan 35 – 55, bagi batuan granit terluluhawa sederhana (Gred III) adalah dalam lingkungan 17 – 35, dan bagi batuan granit terluluhawa tinggi (Gred IV) adalah kurang daripada 17. Manakala, bagi batuan granit terluluhawa keseluruhan (Gred V) dan tanah baki (Gred VI), tidak memberikan nilai lantunan tukul Schmidt. Kaedah ini boleh dijadikan sebagai kaedah yang sangat berguna di lapangan bagi menentukan tahap luluhawa singkapan batuan.

Kata kunci: Granit, gred luluhawa, profil luluhawa, ujian lantunan tukul Schmidt

INTRODUCTION

According to Moye, 1955 and Ruxton & Berry, 1957, weathering profiles in rocks are derived from the geological classification for engineering applications. Weathering profiles are characterized according to their classified weathering grades. There are some properties to be considered in classifying weathering grades. Indeed, in volcano and sedimentary formations there are significant lateral as well as vertical variations, where the original rock type greatly influences the rate of weathering, according to the view by Nahon (1986). According to Umar & Ibrahim (1997), the range of velocities representing grades and indices of weathered rocks and soils can be determined from the in situ seismic surveys at the field. Weathering is an essential process that reduces the mechanical strength of rock material and rock mass at shallow depths from the surface through chemical and physical weathering, as stated by Arikan & Aydin, 2012.

However, defining weathering profile of an outcrop requires identification and judgement of the geologist

0126-5539; 2682-7549 / Published by the Geological Society of Malaysia.

on site and can differ according to each individual's observations. When conducting engineering works, this is important information for the desk study for engineering planning which involves slope stability as well as other engineering purposes. Slope failures, erosion, and landslides often happen in areas that are strongly affected by weathering, and weathering is an environmental factor that impacts recent as well as historical sites (Arikan & Aydin, 2012). In granites, the weathering profile is always much deeper when compared to sedimentary and metamorphic rocks. Most of the proposed weathering profile models are concerned with granitic rocks according to Koita *et al.*, 2013.

According to Abad *et al.*, 2014, one of the most important challenges in the study of slope stability, foundation, and excavation in rocks is understanding the weathering grades. This issue is especially important in tropical climates, where intense weathering produces thick weathering profiles. Therefore, describing the weathering profile involves an understanding of the weathering process of rock exposures of an area. Therefore, many studies have been conducted to achieve the classification of weathering grades. Abad *et al.* (2014) stated that weathering classification schemes are mostly proposed based on some important factors such as the condition and appearance of the rock material (e.g., its friability), the weathered materials engineering properties, the condition of individual minerals (e.g., the extent of micro-cracking), the degree of staining of joint surfaces and/or the extension of the staining from joints into the rock, and alterations to the mineral composition (e.g., the appearance of new minerals and disappearance of existing ones).

A study estimating the degree of weathering of metamorphic rocks from Malaysia using Schmidt hammer rebound test was conducted by Arifin *et al.* (2009) in which the quantification of the weathering grade of rock material is explained, and the linear relationship to the degree of weathering is determined. Goh *et al.*, 2017 states that a mean of quantification of rock material strength can be identified using the Schmidt hammer rebound test.

This study aims to estimate the degree of the weathering grade of granite based on Schmidt hammer rebound tests at Paya Terubong, Pulau Pinang. The area covered is located on Penang Island, a northern island of Malaysia. In this study, the Schmidt hammer rebound values were used to estimate the grade of weathering. The results of the study presents Schmidt hammer rebound test values for the different degree of weathering grades within the weathering profile of granite, as well as demonstrating a useful method for the determination of the degree of weathering in the field.

OVERVIEW OF STUDY AREA

The study area is located at Paya Terubong, Pulau Pinang with coordinate of N 5° 21' 8.24", E 100° 16' 33.16". Based on the Department of Mineral and Geoscience Malaysia (JMG) map of year 2006, the granitic rock in Paya Terubong is composed of medium–grained to coarse–grained biotite granite with microcline. The geology of Paya Terubong forms part of the South Penang Pluton (SPP) and comprises of coarse–grained and medium–grained porphyritic muscovite–biotite granite. Figure 1 shows the geological map of Penang Island modified after JMG, 2006. Figure 2 shows the

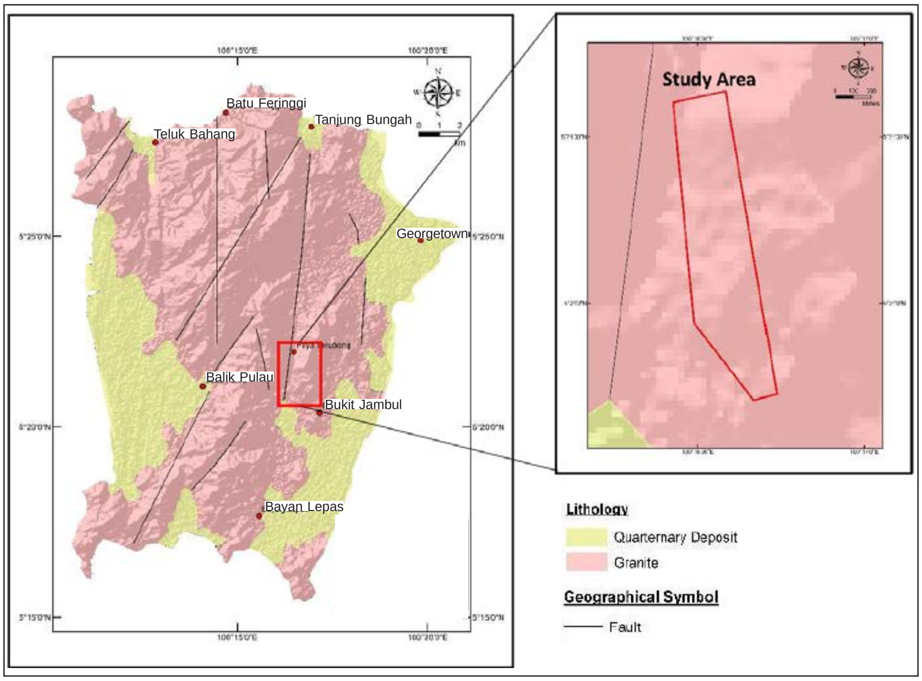

Figure 1: Geological map of Penang Island (modified after Department of Mineral and Geoscience Malaysia (JMG), 2006).

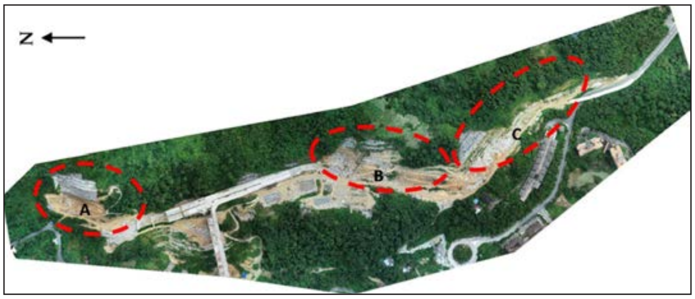

Figure 2: Aerial photo of the study area. Circled areas indicate the locations of *in-situ* Schmidt hammer rebound test done on granitic rock.

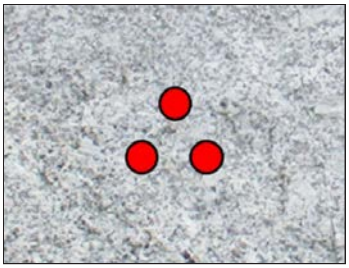

Figure 3: Three blows of *in–situ* Schmidt hammer rebound test done repeatedly at each point.

aerial photo of the study area taken using unmanned aerial vehicle (UAV).

The study area is divided into 3 locations named as location A, location B and location C. The rock outcrop at location A is 150 meters long with a width of 12 meters, at location B it is 95 meters long with a width of 10 meters and at location C, is 70 meters in length and width is 8.5 meters.

METHODOLOGY

The weathering grades of granite in the study area is defined through observation based on the weathering grade classification system of ISRM, 2015 as shown in Table 1. The weathering profile is divided into six (6) weathering grades and classified based on the state of weathering, the rock discoloration, and joint conditions.

Schmidt hammer test is a non–destructive method to estimate the uniaxial compressive strength (UCS) of rock material. According to Aydin & Saribiyik (2010), the rebound hammer test is classified as a hardness test based on the principle that the rebound of an elastic mass depends on the hardness of the surface against which the mass impinges.

The *in–situ* Schmidt hammer rebound test were conducted three times for each point in every grade of weathering to obtain more accurate data. Figure 3 shows the typical procedure in collecting the Schmidt hammer rebound data.

Previous studies had proposed the approximate range values of Schmidt hammer rebound test to determine the weathering grade classification of granite. Table 2 shows the comparison between each range of values proposed.

RESULTS AND DISCUSSION

The results comprise of weathering profiles of the ourcrops in the study area and the *in–situ* Schmidt hammer rebound values of every weathering profile.

Weathering profile of the study area

The results of the tests on rock outcrops in the study area can be divided into 4 weathering zones. The analysis was carried out by constructing several graphs

Table 1: Weathering grade classification system suggested by ISRM (2015).

Term	Class	Description
Sound rock (SR)	I	No visible sign of matrix weathering; some rock discoloration may be presented along main discontinuities.
Slightly weathered rock (SW)	II	Discoloration of rock indicates beginning of rock matrix weathering and along discontinuity surfaces. All rock matrices can be discoloured by weathering and can be slightly softer externally than in sound condition.
Moderately weathered rock (MW)	III	Less than half of rock matrix is decomposed or disintegrated to soil conditions. Sound or discoloured rock is present forming discontinuous zones or as corestones.
Highly weathered rock (HW)	IV	More than half of rock matrix is decomposed or disintegrated to soil conditions. Sound or discoloured rock is present forming discontinuous zones or corestones.
Completely weathered rock (CW)	V	All rock matrices are decomposed or disintegrated to soil conditions. Original structure of rock mass is commonly preserved.
Residual Soil	VI	All rocks are transformed into soil. Geological structure of rock mass is destroyed. There is a great volume of variation but no significant soil transport is present.

Table 2: Comparison of weathering grade classification based on Schmidt hammer rebound values.

Reference	Weathering Grade	Schmidt Hammer Rebound Range Value (R)
Brand & Phillipson (1984)	I	N/A
	II	>45
	III	25 – 45
	IV	<25
	V	No Rebound from Schmidt hammer
	VI	N/A
Yunus *et al.* (2010)	I	>54
	II	37 – 54
	III	17 – 37
	IV	N/A
	V	N/A
	VI	N/A

to identify the degree of weathering of the exposed outcrops. The exposed outcrops in the study area show several weathering profiles, as the following:

a) Weathering profile of grade II – III;
b) Weathering profile of grade III – IV;
c) Weathering profile of grade IV – V;
d) Weathering profile of grade VI (residual soil).

Weathering profile of grade II – III

This profile shows slightly weathered to moderately weathered granite. The outcrop shows some discoloration at the joint surface and slight disintegration of minerals can also be seen. Figure 4 shows the weathering profile of grade II – III. Meanwhile, the graph in Figure 5 shows the *in*–situ Schmidt hammer rebound data collected at the profile. The maximum rebound value (R_{max}) and minimum rebound value (R_{min}) for this profile is 59 and 15 respectively.

Figure 5 is the result of the field test in which the values of Schmidt hammer rebound is plotted vs the position of blows in the study area, and it includes a total of 155 blow numbers at different points with an interval of 3 to 5 meters between each point.

Weathering profile of grade III – IV

This profile shows moderately weathered to highly weathered granite. Discoloration can be observed along the outcrop and disintegration of minerals can be seen. Figure 6 and 7 show the weathering profile of grade III – IV and graph of *in*–situ Schmidt hammer rebound data collected on the profile, respectively. The maximum rebound value (R_{max}) and minimum rebound value (R_{min}) for the profile is 39 and 11, respectively. The test was conducted at 98 locations to determine the degree of weathering.

Figure 4: Overview of weathering profile of grade II – III at circle A area of Figure 2.

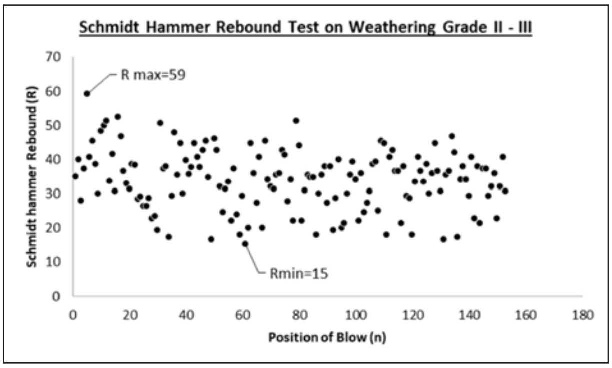

Figure 5: Graph of *in*–*situ* Schmidt hammer rebound test values vs position of blows, on weathering grade II – III; R_{max} = 59, R_{min} = 15.

Figure 6: Overview of weathering profile of grade III – IV at circle B area of Figure 2.

Figure 8: Overview of weathering profile of grade IV – V at circle C area of Figure 2.

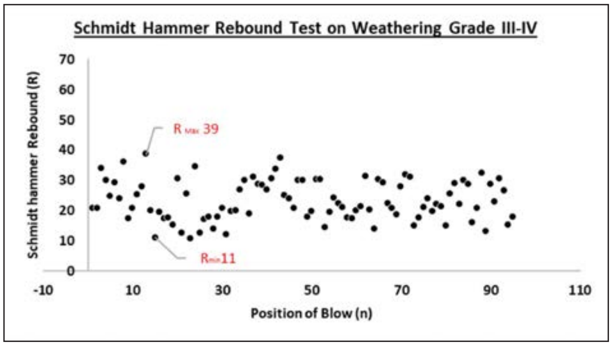

Figure 7: Graph of *in–situ* Schmidt hammer rebound test values vs position of blows, on weathering grade III – IV; R_{max} = 39, R_{min} = 11.

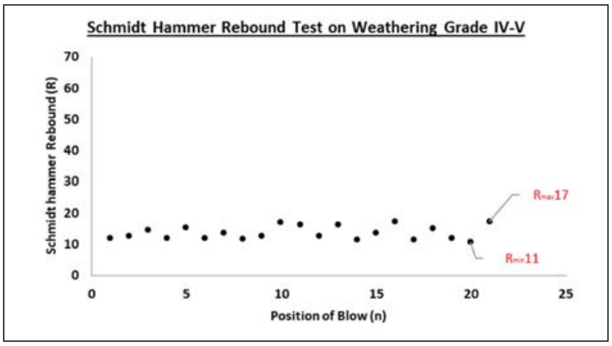

Figure 9: Graph of *in–situ* Schmidt hammer rebound test values vs position of blows, on weathering grade IV – V; R_{max} = 17, R_{min} = 11.

Weathering profile of grade IV – V

This profile shows highly weathered to completely weathered granite. Discoloration can be seen at most of the outcrop and the minerals are highly disintegrated. Dents on the surface of rock can be seen due to the impact of *in–situ* Schmidt hammer rebound test. Figure 8 shows the weathering profile of grade IV – V and Figure 9 shows the graph of *in-situ* Schmidt hammer rebound data collected on the profile. The maximum rebound value (R_{max}) and minimum rebound value (R_{min}) for the profile is 17 and 11, respectively. There were 22 point of blow that classify the degree of weathering in this zone.

Weathering profile of grade VI (residual soil)

This profile is identified as residual soil where all the rock has completely disintegrated into soil. Figure 10 shows the weathering profile of grade VI (residual soil). No graph is constructed as no *in–situ* Schmidt hammer rebound data can be collected at the profile.

Figure 10: Overview of weathering profile of grade VI (residual soil) at circle A area of Figure 2.

Based on the graphs plotted for each of the weathering profile, the range values of *in–situ* Schmidt hammer rebound test are proposed for each weathering grade of granite. The values are interpreted based on the distribution of Schmidt hammer rebound data on the following weathering profiles. Several data that are considered as random error are ignored from the proposed values. Figure 11 shows the range of values of Schmidt hammer rebound data for weathering grades of granite.

Previous researchers such as Brand & Phillipson, 1984 and Yunus *et al.*, 2010 have stated the results of similar studies as in Table 2. In addition, the determination of weathering degree has also considered field observations

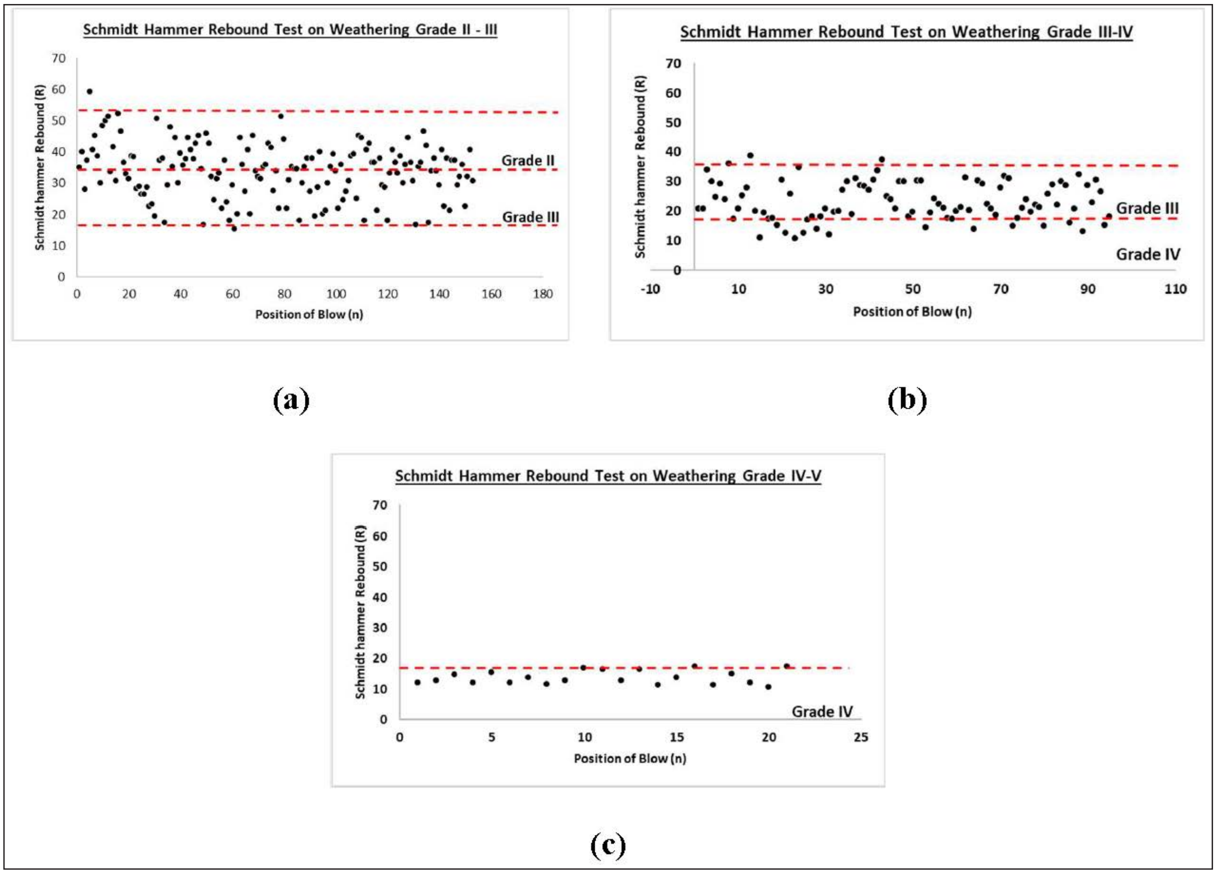

Figure 11: Graph showing the range value of *in–situ* Schmidt hammer rebound test (R) for the different weathering grades.

Table 3: Proposed values of *in–situ* Schmidt hammer rebound test for weathering grade classification for granite at Paya Terubong, Penang, Malaysia.

Term	Weathering Grade	Schmidt Hammer Rebound Test Value (R)
Fresh Granite (F)	I	>55
Slightly weathered Granite (SW)	II	35-55
Moderately weathered Granite (MW)	III	17-35
Highly weathered Granite (HW)	IV	<17
Completely weathered Granite (CW)	V	No rebound
Residual Soil	VI	N/D

N/D : Not determinable

and also the classification of weathering degree by ISRM, 2015 as in Table 1. The results of this study can be concluded that the Schmidth hammer rebound values for the different degrees of weathering in the study area are as follows:

(a) Weathering grade II – III,
$R_{III} = 17 – 35$, $R_{II} = 35 – 55$
(b) Weathering grade III – IV,
$R_{IV} = 0 – 17$, $R_{III} = 17 – 35$
(c) Weathering grade IV – V,
$R_{IV} = 0 – 17$
d) No rebound data for grade V.

Based on the range value of *in–situ* Schmidt hammer rebound test on the weathering profile, the proposed values of *in–situ* Schmidt hammer rebound test for each weathering grade of granite are shown in Table 3.

CONCLUSION

The results of this study have successfully determined the relationship between the value of Schmidt hammer rebound values with the degree of weathering of the study area. The results of this study can be used as a method to determine the degree of weathering of a rock outcrop. The degree of weathering of rock outcrops is one of the important elements in determining the level of rock slope stability. Apart from determining the degree of weathering by observation of the physical condition of the rocks and minerals in the rocks, Schmidt hammer rebound is an excellent method which can provide rock strength values. This paper determined the relationship between the *in–situ* Schmidt hammer rebound test and the weathering grades of a granite weathering profile. The results of this study indicate that Schmidt hammer rebound test for Grade I is greater than 55, Grade II is ranging from 35 – 55, Grade III is ranging from 17 – 35, and Grade IV is less than 17. For Grade V, there is no rebound data that can be collected and Grade VI is identified as residual soil.

ACKNOWLEDGEMENTS

The author would like to express their gratitude to Perunding GEA Sdn Bhd and Yuta Maju Sdn Bhd for the approval on publishing the data for research paper purposes. The authors are also grateful to the two anonymous reviewers for their comments.

AUTHOR CONTRIBUTIONS

In this study, the geological field work was conducted by MSH together with MAG. MRU determined the general geology of the study area as well as the site specific geology. AGMR supervised the in-situ Schmidt hammer testing together with MAG. Interpretation of the results where a correlation of the weathering grades with the Schmidt Hammer rebound values was also conducted by AGMR and MAG. The first draft of the manuscript was prepared by MSH. The manuscript was reviewed by AGMR and MAG with input from MRU.

CONFLICT OF INTEREST

The authors have no conflicts of interest to declare that are relevant to the content of this article.

REFERENCES

Abad, A.N.K.S.V., Mohamad, E.T., Komoo, I. & Kalatehjari, R., 2014. A typical weathering profile of granitic rock in Johor, Malaysia based on joint characterization. Arabian Journal of Geosciences, 8, 2191-2201.

Arifin, M.H., Rafek, A.G. & Goh, T.L., 2009. The use of Schmidt rebound hammer as a method to estimate the degree of weathering for metamorphic rocks from Malaysia. Regional Conference on Environmental and Earth Resources, August 2009, Kuantan, Pahang.

Arikan, F. & Aydin, N., 2012. Influence of weathering on the engineering properties of dacites in Northeastern Turkey. ISRN Soil Science, 2012, 1-15.

Aydin, F. & Saribiyik, M., 2010. Correlation between Schmidt hammer and destructive compressions testing for concretes in existing buildings. Scientific Research and Essays, 5(13), 1644-1648.

Brand, E.W. & Phillipson, H.B., 1984. Site investigation and geotechnical engineering practice in Hong Kong. Geotechnical Engineering, 15(2), 97-153.

Department of Mineral and Geoscience Malaysia (JMG), 2006. Geological traverse survey report (Penang Island) – (Volume 14).

Goh, T.L., Nur Amanin, M., Mohd Sharul, M.N., Abdul Ghani, R., Ailie, S.S., Azimah, H., Lee, K.E. & Foong, S.Y., 2017. Uniaxial compressive strength of Antarctic Peninsula rocks: Schmidt hammer rebound test. Sains Malaysiana, 46(5), 677–684.

ISRM, 2015. The complete ISRM suggested methods for rock characterization, testing and monitoring: 2007-2014. In: Ulusay, R. & Hudson, J.A., (Eds.), Orange Book. Springer International Publishing, Ankara, Turkey. 293 p.

Koita, M., Jourde, H., Koffi, K.J.P., Da Silveira K.S. & Biaou, A., 2013. Characterization of weathering profile in granites and volcanosedimentary rocks in West Africa under humid tropical climate conditions. Case of Dimbokro Catchment (Ivory Coast). J. Earth Syst. Sci., 122(3), 841-854.

Moye, D.G., 1955. Engineering geology for the snowy mountains scheme. J. Inst. Eng., 27(10–11), 287–298.

Nahon, D.B., 1986. Evolution of iron crusts in tropical landscapes. In: Colman, S.M. & Dethier, D.P., (Eds.), Rates of chemical weathering of rocks and minerals. Academic Press, Orlando, Florida. 169–191.

Ruxton, B.P. & Berry, L., 1957. Weathering of granite and associated erosional features in Hong Kong. Geol. Soc. Am. Bull., 68(10), 1263–1292.

Umar, H. & Ibrahim, K., 1997. Seismic velocity and ultrasonic characteristics of granite weathering profile at Km 39.9 Kuala Lumpur-Karak Highway. Sains Malaysiana, 26(1), 19-31.

Yunus, N.B.M., Rafek, A.G., Goh, T. L., & Arifin, M.H., 2010. Analisis pengkuantitatifan gred luluhawa bahan batuan granit dengan ujian tukul Schmidt: Contoh kajian di Malaysia. Warta Geologi, 36, 118.

Manuscript received 9 November 2021;
Received in revised form 25 February 2022;
Accepted 7 March 2022
Available online 26 April 2022

DOI : https://doi.org/10.7186/wg481202204

What makes a hot spring, hot?

Nurul Afiqah Rosli[1], Mohammad Noor Akmal Anuar[2], Muhammad Hasiib Mansor[2], Nur Syazwani Izzati Abdul Rahim[2], Mohd Hariri Arifin[2,*]

[1] Geosciences Department, Universiti Teknologi PETRONAS, Persiaran UTP, 32610 Seri Iskandar, Perak, Malaysia
[2] Department of Earth Sciences and Environment, Faculty of Science and Technology, Universiti Kebangsaan Malaysia, 43600 Bangi, Selangor, Malaysia
* Corresponding author emil address: hariri@ukm.edu.my

Abstract: Hot springs naturally are groundwater that emerges to the surface after being heated up by geothermal activities. There are various classifications of hot springs according to the surface temperature. Still, in Malaysia, it is referred to as the spring that is higher than an average body temperature or 40 °C and above. Two types of hot spring origin are volcanic and non-volcanic sources. The Quaternary magmatic intrusion of Maria volcanic complex in Sabah is the only volcanic-related hot spring. Meanwhile, Sungai Klah, Ulu Slim, Gadek, and other hot springs in Malaysia originated from regional granite intrusion that slowly cooled down since the Triassic period. In Peninsular Malaysia, there is a geological trend of hot springs distribution based on three different intrusion and localities of granite batholiths: Eastern, Central and Western belts of granite. Tectonically, most of these hot springs are associated with fault zones related to highly fractured and deep-seated fault areas with high permeability host rock, such as Bok Bak Fault. Later it can conduit meteoric water to seep deep beneath the subsurface and be subjected to a high geothermal gradient zone. High dissolved minerals in the hot springs are beneficial for balneotherapy, while the excess heat and brine can be harnessed into electrical energy. The development of geothermal potential in Malaysia is still unhurried compared to our neighbouring countries, for example, Thailand's Fang Geothermal Power Plant is a non-volcanic hot spring with a sound temperature of 130°C which can generate 300 kW of electricity. Lastly, effort has been made by researchers in gathering the data on hot spring distribution in Malaysia which can be viewed with just a click. A new app is developed for Android user named Malaysia's Hot Springs that can be freely downloaded from the 'Apps Store' in hope that the application can serve as hot springs tourism and publication reference purposes.

Keywords: Hot springs, Malaysia, geothermal

INTRODUCTION

Do you ever wonder why the temperature of groundwater seeping to the surface, commonly called hot springs, can reach up to a boiling point? Where is the source of heat that influenced the temperature of the water? How hot must the water be before it can be classified into the hot spring category? And what is the future of geothermal energy in Malaysia? Hot springs are heated by the geothermal heat which originates from the Earth's interior. Geothermal energy through hot springs is one of the renewable energy sources that could be harnessed to supply electricity and generate heat. Many hot springs have been found in Malaysia and therefore, the need for more research on geothermal energy particularly from hot springs is vital to fully maximise its potential as an energy source that will benefit the economy of this country in a long run.

DEFINITION

In general, a hot spring is a natural occurrence where heated groundwater emerges on Earth's surface. Its temperature is higher than a body temperature and ranges from 40 °C and above. Apart from the high temperature, the water is also filled with very high concentrations of dissolved minerals such as calcium, sodium, sulphate, chloride, and silica.

SOURCE OF HEAT

The formation process of a hot spring can be answered by investigating the source of its occurrence. An increase in temperature happens due to the groundwater being heated up by the intrusion of magmatic bodies. It then rises to the surface through faults and fractures once it has absorbed enough heat to become lighter than the overlying water. This event is related to volcanic eruptions and commonly

0126-5539; 2682-7549 / Published by the Geological Society of Malaysia.

occur near volcanoes. Therefore, this type of hot spring is classified as the volcanic origin. Hot springs of volcanic origin can be found in East Malaysia such as in Apas Kiri, Tawau, Sabah as shown in Figure 1. Current finding of the geochemistry of Sabah and Sarawak hot springs can be accessed in Anuar *et al*. (2021).

On the other hand, hot springs of non-volcanic origin such as the hot spring in Sungai Klah, Perak, shown in Figure 2, can be explained using the cooling magma and geothermal gradient model (Baioumy *et al.*, 2015). By referring to Figure 3, the magmatic intrusions represent the cooling magma that gives rise to the temperature of the surrounding rocks. Over time, these granitic bodies will be embedded in the Earth's crust and continuously distribute the heat after it is solidified due to the thermal gradient. According to this model theory, researchers look into these three components when analysing hot springs of non-volcanic origin: location of the hot spring, the proximity to granitic intrusion and the distance to major faults or fractured zones.

Generally, temperature increases with depth, therefore, at greater depths where the rocks are so hot, the heat will be distributed to the groundwater, which will eventually make its way up to the surface through faults and fractures. Thus, the heated water that forms hot springs comes from the surface water that penetrated the subsurface to a great depth where the temperature is high, or from the groundwater stored in the aquifers.

In Malaysia, there are over 60 known hot spring sites and more to be discovered (Chow *et al.*, 2010).

Figure 1: An example of a hot spring of volcanic type origin is Apas Kiri, Tawau Hot Spring, Sabah.

Figure 2: An example of a hot spring of non-volcanic origin is Sg. Klah Hot Spring, Perak.

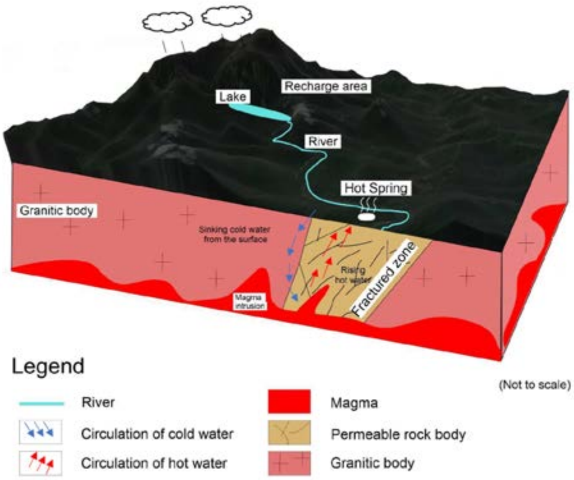

Figure 3: A schematic diagram illustrating the formation of hot spring of non-volcanic origin.

The majority of these hot springs are of non-volcanic origin due to the geographical location of Peninsular Malaysia that is located far from the Ring of Fire and has no active volcanic activities. The highest temperature of hot spring water measured in Peninsular Malaysia is at Sungai Klah Hot Springs, Perak where the temperature can reach 100.2°C. You can even boil eggs in the water.

GEOLOGICAL DISTRIBUTION

The geological distribution of hot springs in Peninsular Malaysia is shown in Figure 4. The distribution of hot springs is concentrated on the west coast of Peninsular Malaysia. It forms a northnorthwest-southsoutheast (NNW-SSE) trend aligned with the main tectonic trend of Peninsular Malaysia.

Researchers have found that most hot spring spots are concentrated near the fault zones. Peninsular Malaysia has numerous major faults, such as Bok Bak Fault, Bukit Tinggi Fault, Kuala Lumpur Fault, Lebir Fault, Seremban Fault, Kisap Fault and Galas Fault. These faults are correlated with hot springs in Peninsular Malaysia within the Eastern and Western belt. Hot springs are usually found in the surrounding area of faults, which are fractured rocks that are permeable, allowing water to flow within the crust. The fluids coming from the highlands are caught by the porous, highly fractured damage zone, which leads them to the surface, explaining the relationship between hot springs and fault occurrence (Taillefer *et al*., 2018).

This is explainable as fractures and faults act as the pathway for meteoric water to flow deep inside the subsurface where the temperature is intense. Hot springs commonly exist in low-lying areas such as swamps, riverbeds, and bedrock surfaces. Given that hot springs occur in these accessible areas, it gives a massive advantage for the developer in planning and utilising the source for the greater good.

BENEFITS AND ADVANTAGES

Continuous efforts have been made in developing hot spring areas into becoming a tourist spot as this heated water has been well known for centuries for its health benefits. One widespread practise in treating illness is balneotherapy, where the body is immersed in mineral-rich water. Hot springs water contains an abundance of dissolved minerals such as sodium, calcium, sulphate, chloride, and silica. This mineral-rich water is believed to have soothing effects on the human body to relieve muscle pain and stressed joints (Erfurt, 2011).

Soaking your body in the warm water of the hot spring is also relaxing and brings tranquillity to your mind. Other than health benefits, hot springs are used to heat spaces, just like an electric heater but it is environmental-friendly and cost-saving. Water from hot springs can also be used for your everyday home purposes such as bathing and washing clothes. On a larger scale, the steam coming out of hot springs is helpful to rotate turbines that could generate electrical energy.

GEOTHERMAL ENERGY

Geothermal is the terrestrial generated heat of the Earth. It is derived from residual energy from Earth's formation and the decay of the radioactive elements in the crust, then transferred to the subsurface by conduction and convection (Tester *et al*., 2006). Throughout the process, water is included as part of a water cycle that comes from rain and snow seeping deep inside the interior portion of the Earth's crust. Upon heating, this groundwater could rise again, emerged with high pressure and temperature to the surface and known as a hot spring. Thus, it is capable of harnessing energy called geothermal energy. For centuries, people have been utilising this energy source for home use, and it has now evolved into the source for generating electricity. As a reference, our neighbour country, Indonesia, has one of the largest geothermal power plants, named Sarulla Geothermal Power Plant, as shown in Figure 6. This fantastic project can supply electricity to 2.1 million households and offset about 1.3 million tonnes (Mt) of carbon dioxide emissions a year (NS Energy, n.d.). Thus, geothermal energy is a renewable energy that is capable of generating a tremendous amount of power supply with lesser pollution to the air!

Can hot springs of non-volcanic origin be utilised to generate electricity? The answer is yes. Let us look into one of the famous non-volcanic hot springs in Thailand that can generate 300 kW of electricity, namely Fang Hot Spring, located in the Chiang Mai province. The water temperature can reach up to 130 °C - enough to generate clean energy for distribution for daily use.

The initiative to turn this area into Fang Geothermal Power Plant started in 1989 by the Electricity Generating Authority of Thailand (EGAT) and it is still well-maintained now. According to Richter (2016), the 300 kW geothermal power plant uses binary cycle technology. It distributes 1.2 million kWh per year as it is linked to the local distribution grid system of the Provincial Electricity Authority (PEA). A binary cycle power plant is a type of geothermal power plant that allows cooler geothermal reservoirs. It is a closed system that uses a second working fluid with a much lower boiling point than water. The geothermal fluid in the form of water vapor and working fluid such as hydrocarbon go through a heat exchanger, where the working fluid converts to vapor and drives the turbines. The cooled water vapour is then released back into the underground reservoirs so the new cycle can begin. Over the years, the hot spring area has expanded into multipurpose facilities such as recreational area, spa, bathtub, and bathrooms to attract visitors worldwide. In Figures 7 and 8, our team collaborated with an industrial partner to visit the power plant in 2018. It amazed us that Thailand has been developing these geothermal resources for years and can supply sufficient energy for the country.

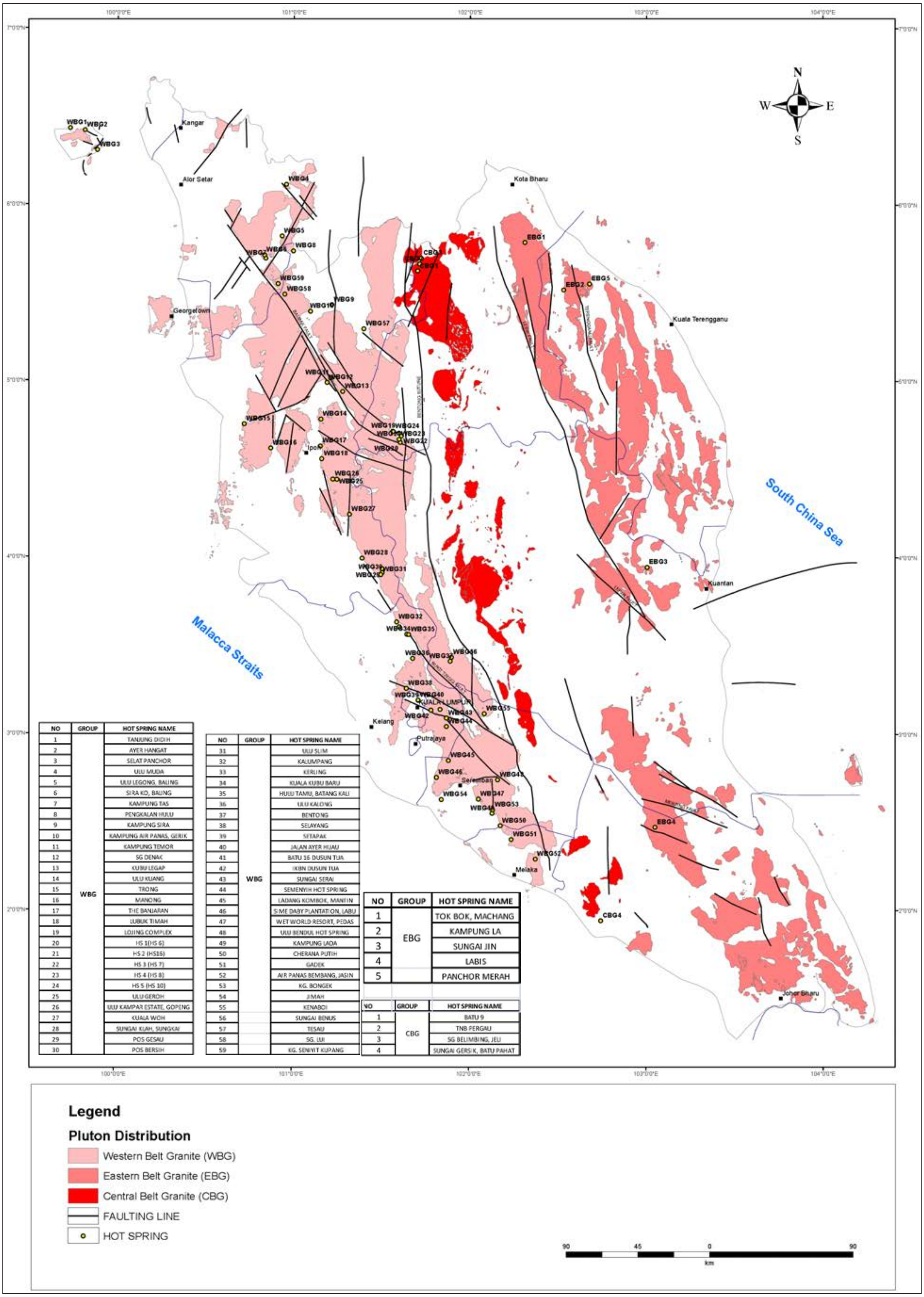

NO	GROUP	HOT SPRING NAME
1	WBG	TANJUNG DIDIH
2		AYER HANGAT
3		SELAT PANCHOR
4		ULU MUDA
5		ULU LEGONG, BALING
6		SIRA KO, BALING
7		KAMPUNG TAS
8		PENGKALAN HULU
9		KAMPUNG SIRA
10		KAMPUNG AIR PANAS, GERIK
11		KAMPUNG TEMOR
12		SG DENAK
13		KUBU LEGAP
14		ULU KUANG
15		TRONG
16		MANONG
17		THE BANJARAN
18		LUBUK TIMAH
19		LOJING COMPLEX
20		HS 1(HS 6)
21		HS 2 (HS16)
22		HS 3 (HS 7)
23		HS 4 (HS 8)
24		HS 5 (HS 10)
25		ULU GEROH
26		ULU KAMPAR ESTATE, GOPENG
27		KUALA WOH
28		SUNGAI KLAH, SUNGKAI
29		POS GESAU
30		POS BERSIH

NO	GROUP	HOT SPRING NAME
31	WBG	ULU SLIM
32		KALUMPANG
33		KERLING
34		KUALA KUBU BARU
35		HULU TAMU, BATANG KALI
36		ULU KALONG
37		BENTONG
38		SELAYANG
39		SETAPAK
40		JALAN AYER HIJAU
41		BATU 16 DUSUN TUA
42		IKBN DUSUN TUA
43		SUNGAI SERAI
44		SEMENYIH HOT SPRING
45		LADANG KOMBOK, MANTIN
46		SIME DABY PLANTATION, LABU
47		WET WORLD RESORT, PEDAS
48		ULU BENDUL HOT SPRING
49		KAMPUNG LADA
50		CHERANA PUTIH
51		GADEK
52		AIR PANAS BEMBANG, JASIN
53		KG. BONGEK
54		JIMAH
55		KENABOI
56		SUNGAI BENUS
57		TESAU
58		SG. LUI
59		KG. SENIYIT KUPANG

NO	GROUP	HOT SPRING NAME
1	EBG	TOK BOK, MACHANG
2		KAMPUNG LA
3		SUNGAI JIN
4		LABIS
5		PANCHOR MERAH

NO	GROUP	HOT SPRING NAME
1	CBG	BATU 9
2		TNB PERGAU
3		SG BELIMBING, JELI
4		SUNGAI GERSIK, BATU PAHAT

Figure 4: The distribution map of hot springs in Peninsular Malaysia. Source: Arifin (2017).

Figure 6: An aerial image of the 330 MW Sarulla geothermal power plant located in North Sumatra, Indonesia.
Source: Richter (2018).

DATA WITHIN REACH

This is an era where every piece of information is attainable with just a touch. 'Malaysia Hot Springs' is a mobile app that contains data on every hot spring in Malaysia such as its location, temperature and the distribution of hot springs in Peninsula Malaysia as shown in Figure 5. This app is beneficial and convenient for researchers to collect first-hand data of their study area such as its water temperature and location. A user can easily access the information by downloading the app, and it is free!

CONCLUSION

Hot springs are a natural occurrence where groundwater is heated up at great depths and brought to the surface through cracks, fractures, and faults. The heated water has a temperature higher than our body and is filled with remarkably high concentrations of dissolved minerals. These properties make hot springs famously known to have healing and soothing effects on the human body, thus contributing to hot springs development as one of the geo-tourism attractions. With about 60 hot springs of low to medium temperatures in Malaysia, geothermal energy can be explored and utilised as a renewable energy source. Therefore, further geoscientific investigations should be considered and carried out in supporting the development plans of geothermal energy. It is hoped that Malaysia will fully utilise and generate electricity from it in the future.

ACKNOWLEDGEMENTS

The authors would like to thank Universiti Teknologi PETRONAS for allowing the internship program with Universiti Kebangsaan Malaysia. Special thanks to the Geology program, Department of Earth Sciences and Environment, Universiti Kebangsaan Malaysia management for encouraging us to publish our research work, and to the reviewers for providing helpful comments.

Figure 7: An image of our team in front of the 300 kW Fang Geothermal Power Plant in Thailand.

Figure 8: An image of our team observing and learning briefly about the geothermal power plant.

AUTHOR CONTRIBUTIONS

NAR wrote the original draft and served as an intern. MNAA was responsible for data curation, investigation and conceptualization of model. MHM and NSIAR reviewed hot springs distribution map and the application/map/figures preparation. MHA administred and supervised the overall project, handled data acquisition and curation, investigation, software, formal analysis, funding acquisition, resources and also as corresponding author.

CONFLICT OF INTEREST

The authors declare that we have no conflict of interest in this paper.

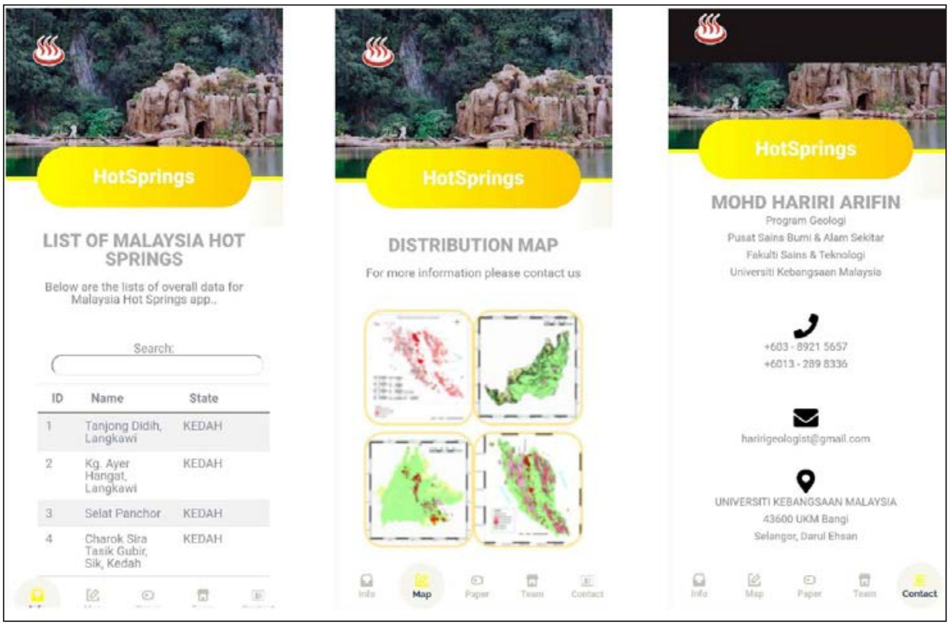

Figure 8: Features that are available in the app are shown. The 'Malaysia Hot Springs' app is downloadable in Androids. For further information, contact Dr. Mohd Hariri Arifin through phone or email.

REFERENCES

Arifin, M.H., 2017. Geothermal potential of hot springs in Peninsula Malaysia from geological, geochemical and geophysical perspectives. Universiti Sains Malaysia. Unpublished PhD thesis.

Anuar, M.N.A., Arifin, M.H., Baioumy, H., & Nawawi, M., 2021. A geochemical comparison between volcanic and non-volcanic hot springs from East Malaysia: Implications for their origin and geothermometry. Journal of Asian Earth Sciences, 217, 104843.

Baioumy, H., Nawawi, M., Wagner, K. & Arifin, M. H., 2015. Geochemistry and geothermometry of non-volcanic hot springs in West Malaysia. Journal of Volcanology and Geothermal Research, 290, 12–22.

Chow, W.S., Irawan, S., & Fathaddin, M., 2010. Hot springs in the Malay Peninsula. Proceedings World Geothermal Congress 2010, Bali, Indonesia, 25-29 April 2010.

Erfurt, P.J., 2011. An assessment of the role of natural hot and mineral springs in health, wellness and recreational tourism PhD dissertation, James Cook University.

N.S. Energy, (n.d.). Sarulla Geothermal Power Plant. https://www.nsenergybusiness.com/projects/sarulla-geothermal-power-plant/.

Richter, A., 2016. Fang geothermal plant in Chiang Mai, model for more to come in Thailand? ThinkGeoEnergy. https://www.thinkgeoenergy.com/fang-geothermal-plant-in-chiang-mai-model-for-more-to-come-in-thailand/.

Richter, A., 2018. 330 MW Sarulla geothermal plant in Indonesia completed with the third unit online. ThinkGeoEnergy. https://www.thinkgeoenergy.com/330-mw-sarulla-geothermal-plant-in-indonesia-completed-with-third-unit-online/.

Taillefer, A., Guillou-Frottier, L., Soliva, R., Magri, F., Lopez, S., Courrioux, G., Millot, R., Ladouche, B. & Le Goff, E., 2018. Topographic and faults control of hydrothermal circulation along dormant faults in an Orogen. Geochemistry, Geophysics, Geosystems, AGU and the Geochemical Society, 19(12), 4972-4995.

Tester, J.W., Anderson, B.J., Batchelor, A.S., Blackwell, D.D., DiPippo, R., Drake, E.M., Garnish, J., Livesay, B., Moore, M.C., Nichols, K., Petty, S., Toksöz, M.N., Veatch, R. W., 2006. The future of geothermal energy - Impact of enhanced geothermal system (EGS) on the United States in the 21st century. MIT, USA. 372 p.

Manuscript received 7 June 2021;
Received in revised form 27 January 2022;
Accepted 28 January 2022
Available online 26 April 2022

CERAMAH TEKNIK TECHNICAL TALK

Geological highlights of Brunei Darussalam (North Borneo) with focus on the "Borneo Amber" record

László Kocsis
Date: 14 December 2021
Platform: Google Meet

Abstract: Since 2014 we have been conducting research on Brunei's Neogene deposits. During our field surveys we discovered some exceptional fossil assemblages. Here, the already published and most remarkable remains are shown to give a taste of ancient biodiversity of the region. Mollusks, cartilaginous fish among them the famous *Otodus megalodon*, late Miocene turtle remains, and microfossils such as pollen and foraminifera will be briefly discussed. Most of these fossils come from the middle to late Miocene shallow marine deposits of the Miri and Seria formations. These beds, however, and also almost all other sedimentary succession in Brunei, often contain fossilized tree resins (amber) as well. These remains are very common and can be fairly abundant in certain layers. Amber comes with different size and color, some are transparent, and others are completely opaque. Often they show the sign of bioerosion, while others contain trapped insects. We collected a large amount of amber, and selected specimens together with modern tree resins were characterized and investigated with different methods (e.g., physical properties, FTIR, $\delta^{13}C$). Most of the results point to maturation differences among the samples, while the FTIR spectrum of over 60 analyzes revealed that all the Brunei ambers were produced by dipterocarp trees Dipterocarpaceae), and no fossil Agathis (Araucariacea) resin has been detected. This is in agreement with the lower abundance of the gymnosperm taxon in the forests of Borneo compared to that of the widespread dipterocarps. From the late middle Miocene to late Miocene a slight decreasing trend in average $\delta^{13}C$ values was detected that can be explained by gradual changes in local environmental conditions (e.g., more precipitation) and/or by increased amount of less mature specimens among the younger samples. In contrast, the Pliocene samples yielded the highest $\delta^{13}C$ values that may link to cooler-drier climate with increased seasonality, probably reflecting the spread of glaciation in the northern hemisphere.

Comments: This talk took place online, using University of Malaya's Google Meet facility. The talk was recorded, and can be viewed at this URL:
https://drive.google.com/file/d/1WT0-HkNswsOSdIi5XPI74im4Q49Knwzg/view?usp=sharing

We had twelve in the audience. The talk covered a lot of ground. Amber is commonly found in Borneo in the Cenozoic sedimentary record, often associated with coal, and also found reworked on modern beaches. Modern tree resins are also commonly found and continuously produced in the region, and can be mixed up with amber. Telling the two apart can be done using physical characteristics, for instance, amber has stronger fluorescence than modern tree resins when exposed to UV light. The talk also covered the geochemistry of both amber and modern tree resins - amber has distinctive FTIR and carbon isotope signatures, as well as distinctive organic geochemistry.

Amber is very often found "across the border" in Sarawak and Sabah, as well as in Kalimantan, so this is an avenue for possible future research. The University of Malaya Geology Department is equipped to participate in this research, since we have a well-equipped organic geochemistry laboratory as well as a Micro-CT which can be used to image and model insects and other organisms or biological particles (pollen?) preserved in amber.

Further reading:

László Kocsis, Anwar Usman, Anne-Lise Jourdan, Syaimaa' Haji Hassan, Nurhazwana Jumat, Dalina Daud, Antonino Briguglio, Ferry Slik, László Rinyu & István Futó, 2020. The Bruneian record of "Borneo Amber": A regional review of fossil tree resins in the Indo-Australian Archipelago. Earth-Science Reviews, 201, 2020, 103005, ISSN 0012-8252.
https://doi.org/10.1016/j.earscirev.2019.103005.
https://www.sciencedirect.com/science/article/pii/S0012825219302004.

Prepared by:
Dr. Nur Iskandar Taib (UM, Retired)
Councillor, Geological Society of Malaysia
28th February 2022

CERAMAH TEKNIK TECHNICAL TALK

The Devonian-Carboniferous boundary in Perlis, NW Peninsular Malaysia: Recording changes in fossil fauna, palaeoclimate and depositional settings

Meor Hakif bin Amir Hassan
Date: 16 December 2021
Platform: Google Meet

Abstract: The Sanai Hill B outcrop, exposed at Kampung Guar Jentik, Beseri district, Perlis, exposes one of the best-preserved Devonian-Carboniferous boundary successions in Malaysia. A new geologic map for the locality is presented, which is based on better exposure of the outcrop due to active quarrying, and was constructed using a combination of aerial drone imagery, three-dimensional photogrammetry, Google Earth satellite imagery and traditional field methods. The sedimentary strata include the Silurian Mempelam Limestone, the Lower Devonian Timah Tasoh Formation, the Upper Devonian Sanai Limestone, the Lower Carboniferous Telaga Jatoh Formation and the Lower Carboniferous Chepor Member of the Kubang Pasu Formation. The Devonian-Carboniferous boundary is marked by the contact between the Sanai Limestone and the Telaga Jatoh Formation. It shows an abrupt change from carbonate to siliceous (chert) deposition, with the contact represented by a paraconformity. This unconformity can be correlated to the Devonian-Carboniferous unconformity in the Kanthan Limestone of Perak. It can also be identified in many sections throughout the Western Belt, including in southern Thailand, Langkawi, Kedah, Perak and the Selangor-Kuala Lumpur area. The unconformity can be linked to a eustatic sea level fall at the end of the Devonian.

Comments: This talk took place online, using University of Malaya's Google Meet facility. The talk was recorded, and can be viewed at this URL:
https://drive.google.com/file/d/1md8jD_YSpp-FWN9lDwb9OnfgCLLKwt86/view?usp=sharing

The talk was centered around development of the understanding of the Paleozoic section exposed in Perlis, as more outcrops became available over time. The Sanai Limestone was initially thought to be part of the Ordovician-Silurian Setul Limestone (mainly exposed in Langkawi), but was revealed to be of Late Devonian age through the study of conodonts and the presence of homoctenid tentaculitoids. There was a lot of interest from the audience, particularly those from the petroleum sector, since drill core retrieved from the Malacca Straits reveals similar rocks. It will take further examination of fossils to determine whether this is the same section. Over 70 people attended this talk, including several from the petroleum industry, and students, mainly from UMK and UM. Dr. Hafzan Eva from UMK asked the students from her class to attend the talk. Since there is much interest on this subject, GSM will organize a seminar on the Paleozoic section of the Western Malay Peninsula in the near future.

Further reading:

Amir Hassan, M.H., 2021. The Devonian-Carboniferous boundary at Guar Sanai, Kampung Guar Jentik, Perlis: An updated map and stratigraphic section. Bulletin of the Geological Society of Malaysia, 71, 57 - 69.

Amir Hassan, M.H., Mustafa, Y.A., Zakaria, M.Z.Z. & Ghani, A.A., 2015. First record of Homoctenus (Tentaculitoidea, Homoctenida) from the Late Devonian of northwest Peninsular Malaysia. Alcheringa: An Australasian Journal of Palaeontology, 39(4), 550-558.

Amir Hassan, M.H., Aung, A-K., Becker, R.T., Rahman, N.A.A., Fatt, N.T., Ghani, A.A. & Shuib, M.K., 2014. Stratigraphy and palaeoenvironmental evolution of the mid- to upper Palaeozoic succession in Northwest Peninsular Malaysia. Journal of Asian Earth Sciences, 83, 60-79.

Aung, A.K., Meor, H.A.H. & Ng, T.F., 2013. Discovery of Late Devonian (Frasnian) conodonts from the "Sanai limestone", Guar Jentik, Perlis, Malaysia. Bulletin of the Geological Society of Malaysia, 59, 93-99.

Prepared by:
Dr. Nur Iskandar Taib (UM, Retired)
Councillor, Geological Society of Malaysia
28th February 2022

CERAMAH TEKNIK TECHNICAL TALK

Distinct element modelling in rock engineering

Boon Chia Weng
Date: 19 February 2022
Platform: Zoom / Facebook Live GSM

The above talk was delivered by Dr Boon Chia Weng (Gamuda) on 19th February 2022, via Zoom/Facebook Live. Some 25 members participated. An abstract of the talk is provided below:

Abstract: The use of the distinct element method is increasingly becoming more widespread in civil engineering projects. The theory and algorithms of the distinct element method were explained in the first half of the presentation. Subsequently, the use of distinct element method (DEM) for jointed rock analysis was being demonstrated. The presentation placed emphasis on capturing the key geological structure of the rock, so that the failure mechanisms could be reflected correctly in the models. Examples were drawn from underground openings and slopes. The presentation included a discussion of the circumstances for which the geological structure could influence the rock bolt forces and reinforcement mechanisms around underground openings. Similarly, for slopes, the presentation showcased how the joint orientation, joint shear strength and boundary conditions of a slope could influence its kinematics.

We thank Dr Boon for his support and contribution to the Society's activities.

Tan Boon Kong
Chairman, Working Group on Engineering Geology
28th February 2022

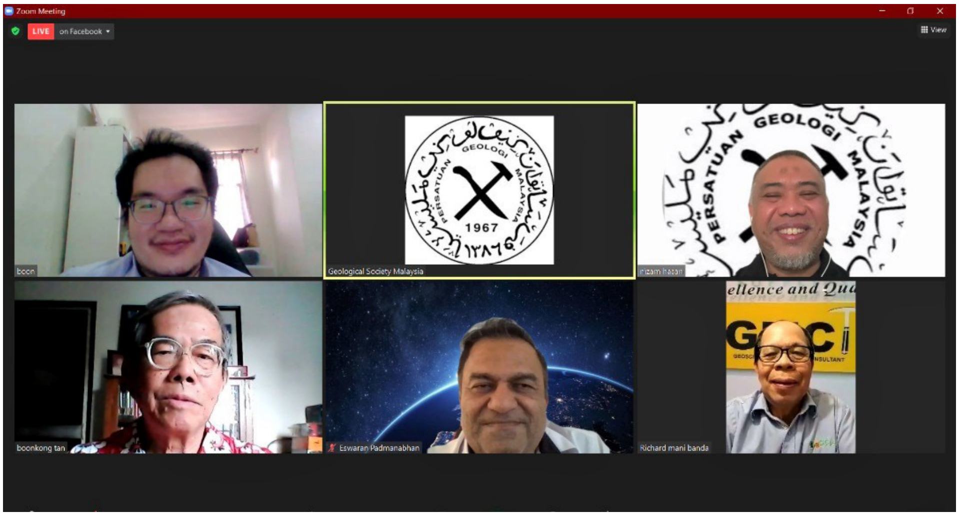

CERAMAH TEKNIK TECHNICAL TALK

Rock slope stability analysis: The selection and modelling issue

Rini Asnida Abdullah
Date: 22 March 2022
Platform: Zoom / Facebook Live GSM

The above talk was delivered by Ir Dr Rini Asnida Abdullah (UTM) on 22nd March, 2022, via Zoom/Facebook Live. Some 45 members participated.

The talk presented some case studies on rock slope failures, including several interesting videos on plane failure, toppling, and rock falls. A case study on rock slope stability analysis in a slate quarry in England was taken from the speaker's Ph.D. thesis in the Univ. of Leeds, UK. Analysis and modelling of rock slope stability include kinematic analysis utilising stereonets, and softwares incorporating the Finite Element Method (FEM) and the Distinct Element Method (DEM).

We thank Dr Rini for her support and contribution to the Society's activities.

Tan Boon Kong
Chairman, Working Group on Engineering Geology
6th April 2022

CERAMAH TEKNIK TECHNICAL TALK

The causes of landslides

Darryl Fong Chew Chung
Date: 13 April 2022
Platform: Zoom

The above talk was delivered by Ir. Darryl Fong Chew Chung (G&P) on 13th April, 2022, via Zoom. Some 30 members participated. An abstract of the talk is provided below.

Abstract: The safety of buildings on hillsites is often a worrying concern especially during heavy or prolonged rainy periods. This talk aims to explain how and why landslides occur. It also provides examples of safe and sustainable hillsite developments.

We thank Ir. Fong for his support and contribution to the Society's activities.

Tan Boon Kong
Chairman, Working Group on Engineering Geology
14th April, 2022

Acknowledgement to Peer Reviewers (2021)

In appreciation of the enormous contribution they make to the Society's publications, we would like to thank the scholars and experts below who have participated in the peer review process of manuscripts submitted for consideration for publication in the Bulletin of the Geological Society of Malaysia and Warta Geologi in 2021:

Abdul Halim Abdul Latiff

Adi Susilo

Ahmad Farid Abu Bakar

Ahmed Mohamed Ahmed Salim

Aiad Ali Hussien Al-Zaidy

Allan J. Filipov

Askury Abd Kadir

Azman bin Abd. Ghani

Azrin binti Azmi

Benson Shadrach Jatau

Che Aziz Ali

Elvaene James

Fauzi Mardan Al-Beyati

Felix Tongkul

Franz L. Kessler

Hamzah Hussin

Hareyani binti Zabidi

Harry Doust

Hennie Fitria Wulandary Soehady Erfen

Herman Darman

Joe Chong

John Jong

John Kuna Raj

Joy Jacqueline Pereira

Kehinde James Ogunmola

Lee Chai Peng

Lim Choun Sian

Maher Mandeel Mahdi

Mazlan Madon

Micheal Scherer

Mohd Hariri Arifin

Muhammad Hafeez Jeofry

Muhammad Hatta Roselee

Muhammad Noor Amin Zakariah

Muhammad Sofi bin Mohammed Nasir

Mustaffa Kamal Shuib

Ng Tham Fatt

Noer El Hidayah binti Ismail

Norbert Simon

Nordiana binti Mohd Muztaza

Nursufiah bte Sulaiman

Peter Lunt

Peter Woodroof

Robert Hall

Robert Shoup

Rohayu Che Omar

Salah Hussain

Salam Al-Dulaimi

Simon Kasidi

Sukonmeth Jitmahantakul

Tan Boon Kong

Thamer Mahdi

Tjipto Prastowo

Vijayan V.V. Rajan

Yasir Bashir

Zuliskandar Ramli

THANK YOU

LAPORAN REPORT

Ringkasan Laporan aktiviti Kumpulan Kerja Kuarternari dan Geologi Marin – Persatuan Geologi Malaysia – 2021

Sepanjang tahun 2021, Kumpulan Kerja Kuarternari dan Geologi Marin yang dipengerusikan oleh En. Abdullah Sulaiman telah menganjurkan beberapa aktiviti di bawah Persatuan Geologi Malaysia dan juga program kerjasama bersama Institut Geologi Malaysia.

Maklumat program yang telah dianjurkan di bawah kelolaan kumpulan adalah seperti di bawah:

GSM FB Live - Kumpulan Kerja Kuarternari dan Geologi Marin & Unit Promosi GSM

Penceramah : Dr. Kamaludin Hassan
Topik : The Quaternary and Climate Change
Tarikh : 23 Ogos 2021
Masa : 1000 - 1200
Medium : FB Live & Zoom
Jumlah peserta/ tontonan : 781 tontonan
Pautan video : https://fb.watch/ajvB65jYtE/

Ringkasan program: Program telah dimulakan dengan ucapan aluan oleh moderator bagi memperkenalkan Dr. Kamaludin Hassan. Seterusnya sesi telah dikemudi oleh Dr. Kamaludin di mana beliau telah berkongsi pengalaman juga dapatan kajian beliau berkaitan deposit kuartenari dan perkaitannya dengan perubahan iklim yang menjadi topik hangat masa kini. Sesi ini diselang-selikan dengan pertanyaan dari para peserta juga perkongsian para peserta terhadap topik yang dibincangkan. Sesi telah dirumuskan dan ditutup oleh moderator sekitar jam 1200 tengahari.

GSM FB Live - Kumpulan Kerja Kuarternari dan Geologi Marin & Unit Promosi GSM

Penceramah : Profesor Dato' Dr. Mokhtar Saidin
Topik : Halatuju Geoarkeologi Negara
Tarikh : 27 Ogos 2021
Masa : 1500 - 1700
Medium : FB Live & Zoom
Jumlah peserta/ tontonan : 2100 tontonan
Pautan video : https://fb.watch/ajvyNEo7Fs/

Ringkasan program: Program telah dimulakan dengan ucapan aluan oleh moderator bagi memperkenalkan YBhg Profesor Dato' Dr. Mokhtar Saidin. Beliau memulakan program dengan berkongsi latar belakang beliau dan juga pencapaian beliau sepanjang beliau terbabit dalam bidang geoarkeologi di mana antara kemuncak pencapaian karier beliau adalah pengenalan kepada tapak sejarah Lembah Bujang di mana ianya menjadi antara bukti penting kepada peradaban manusia di tanah melayu pada ketika itu. Beliau juga berkongsi apakah halatuju bidang ini di masa hadapan dan cabaran-cabaran yang harus ditangani bagi meletakkan bidang geoarkeologi marin pada tahap yang lebih tinggi. Program ini telah diakhiri dengan sesi soal jawab bersama YBhg Profesor Dato' Dr. Mokhtar Saidin.

GSM FB Live - Kumpulan Kerja Kuarternari dan Geologi Marin & Unit Promosi GSM

Penceramah : En. Ruzairy Bin Arbi
Topik : Aktiviti dan Hala Tuju Arkeologi Marin Di Malaysia
Tarikh : 17 September 2021
Masa : 1000 - 1200
Medium : FB Live & Zoom
Jumlah peserta/ tontonan : 898 tontonan
Pautan video : https://fb.watch/ajvwMIebRI/

Ringkasan program: Program ini adalah kesinambungan dari program bersama YBhg Profesor Dato' Dr. Mokhtar Saidin, di mana pada kali ini wakil dari Jabatan Warisan Negara telah dipilih menjadi penceramah jemputan. Program telah dimulakan dengan ucapan aluan oleh moderator bagi memperkenalkan En. Ruzairy Bin Arbi. Beliau memulakan program dengan berkongsi latar belakang beliau dan juga pencapaian beliau sepanjang beliau terbabit dalam bidang arkeologi marin bersama Jabatan Warisan Negara. Seterusnya beliau telah berkongsi pelbagai fakta dan undang-undang berkaitan bidang arkeologi marin dan juga cabaran yang dihadapai oleh Jabatan Warisan Negara dalam memelihara warisan arkeologi marin negara. Program diakhiri dengan sesi soal jawab dan perbincangan berkaitan bidang arkeologi marin bersama para peserta.

GSM FB Live - Kumpulan Kerja Kuarternari dan Geologi Marin & Unit Promosi GSM

Penceramah : A.P. Dr. Edlic Sathiamurthy
Topik : Sundaland LGM to Present Day -
Land Connections & Disconnections, Changing Environment
& River Basin Arrangement
Tarikh : 23 September 2021
Masa : 1500 - 1700
Medium : FB Live & Zoom
Jumlah peserta/ tontonan : 780 tontonan
Pautan video : https://fb.watch/akLrz_zgND/

Ringkasan program: Pentas Sunda telah menjadi tumpuan para pengkaji dari serata dunia untuk lebih memahami perubahan paras laut dan implikasinya terhadap kawasan sekitaran. Sehubungan itu pihak Kumpulan Kerja Kuarternari dan Geologi Marin & Unit Promosi GSM telah menjemput A.P. Dr. Edlic Sathiamurthy untuk berkongsi hasil kajian beliau berkenaan evolusi aliran sungai purba yang berkait rapat dengan evolusi perubahan dasar laut di sekitaran Pentas Sunda. Program telah dimulakan dengan ucapan aluan oleh moderator bagi memperkenalkan A.P. Dr. Edlic Sathiamurthy. Beliau memulakan program dengan berkongsi latar belakang beliau dan juga kajian dan kolaborasi yang telah beliau lakukan sebagai seorang pensyarah dan penyelidik di Universiti Malaysia Terengganu. Beliau telah berkongsi dapatan kajian yang telah beliau lakukan di kawasasn pantai timur Semenanjung Malaysia di mana beliau telah berkongsi bukti-bukti aliran sungai kuno yang menjadi bukti kawasan tersebut pernah berada di daratan suatu masa dahulu. Beliau mengakhiri program beliau dengan menjawab persoalan dan pertanyaan dari para peserta yang hadir pada sesi tersebut.

GSM FB Live - Kumpulan Kerja Kuarternari dan Geologi Marin & Unit Promosi GSM

Penceramah : En. Dhani Irwanto
Topik : Decoding Plato's Narrative to Find Atlantis
Tarikh : 15 Oktober 2021
Masa : 0930 - 1130
Medium : FB Live & Zoom
Jumlah peserta/ tontonan : 2100 tontonan
Pautan video : https://fb.watch/akOiIaBw9d/

Ringkasan program: Kesinambungan dari program berkaitan Pentas Sunda bersama A.P. Dr. Edlic Sathiamurthy, pihak Kumpulan Kerja Kuarternari dan Geologi Marin & Unit Promosi GSM telah berjaya mendapatkan En. Dhani Irwanto atau lebih mesra dengan panggilan Pak Dhani untuk berkongsi kajian beliau berkaitan mitos kota Atlantis dan hubungkait kebarangkalian kewujudan mitos ini di Pentas Sunda suatu masa dahulu. Program telah dimulakan dengan ucapan aluan oleh moderator bagi memperkenalkan En. Dhani Irwanto. Pak Dhani telah memulakan sesi perkongsian dengan memperjelaskan teori–teori berkaitan kota Atlantis dan bagaimana ianya telah direkodkan oleh pengkaji-pengkaji terdahulu. Beliau telah berkongsi dapatan kajian yang telah beliau lakukan di mana beliau memperincikan setiap bukti yang telah beliau temui dan bagaimana ianya selari dengan catatan rekod oleh pengkaji terdahulu. Beliau mengakhiri program beliau dengan menjawab persoalan dan pertanyaan dari para peserta yang hadir pada sesi tersebut.

Disamping itu pihak GSM melalui kumpulan kerja ini juga turut menganjurkan webinar dengan kerjasama pihak IGM seperti maklumat dibawah:

IGM GSM 3rd National Workshop on Coastal and Marine Geology 2021

Tema : Towards Sustainable Coastal and Marine Management
Tarikh : 30 Ogos 2021
Masa : 0800 - 1700
Medium : Zoom
Jumlah peserta : 180 peserta

Ringkasan program: Program 3rd National Workshop on Coastal and Marine Geology, 2021, telah berlansung secara atas talian pada 30 Ogos 2021. Bengkel ini adalah anjuran bersama Persatuan Geologi Malaysia (GSM), Institut Geologi Malaysia (IGM), Jabatan Geosains (UTP), UTP-ERASMUS+ (MARE) dan telah dikendalikan oleh Academy GEX. Bengkel ini telah dihadiri seramai 180 peserta dari pelbagai latarbelakang termasuk para pelajar siswazah dan pasca-siswazah, agensi-agensi kerajaan dan pemain industri yang berkaitan. Bengkel ini telah dimulakan oleh ucapan aluan dari pengarah bengkel P.Geol. En. Mohamad Shaufi Sokiman (M.I.G.M) (UTP) dan kemudiannya disusuli oleh ucapan dari penasihat bengkel iaitu P.Geol. En. Abdullah Sulaiman (F.I.G.M) (JMG). Bengkel seterusnya telah dibuka secara rasmi oleh P.Geol. En. Ahmad Nizam Hasan (F.I.G.M), Presiden Persatuan Geologi Malaysia (GSM).

Mengangkat tema pembangunan lestari zon pesisir pantai, bengkel telah dibahagikan kepada 4 sesi di mana 3 sesi teknikal telah dipecahkan mengikut tema iaitu sesi 1 – (Coastal & Marine Development from Geological Perspective), sesi 2 – (Coastal Issues, Protection and Adaption), sesi 3 – (Coastal Resources & Sustainable Management) dan Sesi 4 (Panel Session). Sesi 1 telah dikemudi oleh P.Geol. Dr. Khaira Ismail (M.I.G.M) (UMT) bersama ahli panel yang terdiri daripada P.Geol. Noran Alwakhir Shaarani (M.I.G.M) (JMG) (Coastal Geological Hazard Mapping), P.Geol. A.P. Dr. Hasrizal Shaari (M.I.G.M) (UMT) (Coastal Pollution), P.Geol. Dr. Ferdaus Ahmad (JMG) (Engineering Geology on Coastal Zone) dan Professor Madya Dr. Edlic Sathiamurthy (UMT) (Delta Environment).

Sesi 2 pula telah dikemudi oleh Dr. Effi Helmy Ariffin (UMT) bersama barisan ahli panel yang terdiri daripada Ir. Iwan Tan Sofian Tan (Dr Nik & Associates Sdn. Bhd.) (Coastal Development Projects & Their Impacts to Coastal Environment), Dr. Lee Hin Lee (NAHRIM) (Sea Level Rise & Impact to Coastal Environment), Dr. Khamarrul Azahari Razak (UTM) (Coastal Hazards) dan Ir. Arman Mokhtar (JPS) (Integrated Coastal Zone Management). P.Geol. Muhammad Mustadza Mazni (M.I.G.M) (JMG) telah mengemudi sesi teknikal terakhir iaitu sesi 3 dimana

sesi ini telah mengumpulkan ahli-ahli panel yang terdiri daripada P.Geol. Dr. Dana a/k Badang (M.I.G.M) (JMG) (Costal resources - Geosite & Geopark), Dr. A. Aldrie Amir (LESTARI – UKM) (Coastal Resources - Mangrove) dan Prof. Dr. Wan Izatul Asma binti Wan Talaat (INOS-UMT) (Marine Spatial Planning) (Law & Regulation).
Bengkel diteruskan dengan sesi perbincangan panel yang telah dikemudi sendiri oleh P.Geol. En. Abdullah Sulaiman (F.I.G.M) (JMG). Sesi perbincangan panel telah disertai oleh Prof. Dr. Wan Izatul Asma binti Wan Talaat (INOS-UMT), Dr. A. Aldrie Amir (LESTARI – UKM) dan Dr. Khamarrul Azahari Razak (UTM). Sesi perbincangan panel menyaksikan pelbagai komen dan pendapat telah dilontarkan oleh ahli-ahli panel berkaitan permasalahan terkini dan jalan penyelesaian yang harus dan sewajarnya diambil bagi memastikan kelestarian pembangunan zon pantai dapat dicapai.
Usai sesi perbincangan panel, para ahli panel dan peserta beralih ke acara penutupan bengkel yang telah dizahirkan oleh P.Geol. Gs. En. Abd Rasid Jaapar, F.I.G.M, FGS, MIGRSM, selaku Presiden Institut Geologi Malaysia. Dalam ucapan penutupan beliau, En. Abd Rasid Jaapar telah menekankan akan kepentingan penglibatan pelbagai pihak dalam menjamin kelestarian pembangunan teutamanya bagi kawasan pesisir pantai di masa hadapan. Sesi seterusnya diakhiri dengan sesi bergambar secara maya bersama para peserta yang hadir.

IGM GSM – SEMINAR ON COASTAL AND MARINE GEOLOGY

Tema : Issues and Challenges of Urban Development on Peatlands in Malaysia
Tarikh : 25 Oktober 2021
Masa : 0830 - 1700
Medium : Zoom
Jumlah peserta : 80 peserta

Ringkasan program: Program Issues and Challenges of Urban Development on Peatlands in Malaysia, telah berlansung secara atas talian pada 25 Oktober 2021. Seminar ini adalah anjuran bersama Persatuan Geologi Malaysia (GSM), Institut Geologi Malaysia (IGM) dan telah dikendalikan oleh Academy GEX. Seminar ini telah dihadiri seramai 80 peserta dari pelbagai latarbelakang termasuk para pelajar siswazah dan pasca-siswazah, agensi-agensi kerajaan dan pemain industri yang berkaitan. Bengkel ini telah dimulakan oleh ucapan aluan dari pengerusi bengkel iaitu P.Geol. En. Fakhruddin Afif Fauzi (M.I.G.M) (JMG). Sesi kemudiannya dimulakan oleh ucaptama Dr. Lulie Melling, Pengarah, Sarawak Tropical Peat Research Institute (TROPI).
Mengangkat tema kepentingan pengurusan tanah gambut, bengkel telah dibahagikan kepada 2 sesi. Sesi 1 telah dikemudi oleh P.Geol Dr. Khaira Ismail (M.I.G.M) (UMT) bersama ahli panel yang terdiri daripada P.Geol. Ahmad Nizam Hasan (F.I.G.M) (GSM) – (Geological Assessment for Urban Development Planning Over Peatlands - Study Case of Selangor State), Malaysian Peatland. Dr. Rohani Shahrudin (UMT) – (Biodiversity & Conservation: Where Are We Now?), P.Geol. Dr. Mohd Hariri Arifin (UKM) (M.I.G.M).
Sesi 2 pula telah dikemudi oleh P.Geol. Mohamad Shaufi Sokiman (M.I.G.M) (UTP) bersama barisan ahli panel yang terdiri daripada En. Wan Aminordin Wan Kamaruddin (JAS) – (Malaysian National Programme for Peatland Fire Prevention), Ir. Som Pong Pichan (JKR) – (Challenges in Site Investigation for Geotechnical Design on Peat Soils) dan Pn. Hasnida Zabidi (JMG) – (Kebakaran Tanah Gambut di Malaysia; Peranan JMG). Sesi diteruskan dengan sesi soal jawab secara maya bersama para peserta.
Acara penutupan bengkel yang telah dizahirkan oleh P.Geol. En. Abdullah Sulaiman (F.I.G.M) (JMG) selaku Pengerusi kepada Kumpulan Kerja Kuarternari dan Geologi Marin (GSM) dan Pengerusi Kumpulan Teknikal Pesisir Pantai dan Geologi Marin (IGM). Sesi seterusnya diakhiri dengan sesi bergambar secara maya bersama para peserta yang hadir.

Untuk perancangan masa hadapan, pihak GSM melalui jawatan kuasa kerja telah merancang beberapa pengisian untuk tahun 2022 seperti dibawah:

1. IGM – GSM - Seminar Deep Seabed Mining (February 2022).
2. IGM - GSM 4th National Workshop on Coastal and Marine Geology 2022 (Perincian maklumat akan dikemaskini dari masa ke semasa).
3. Webinar bulanan (Perincian maklumat akan dikemaskini dari masa ke semasa).

Disediakan oleh,
Mohamad Shaufi Bin Sokiman
Setiausaha, Kumpulan Kerja Kuarternari dan Geologi Marin – Persatuan Geologi Malaysia

LAPORAN REPORT

Building capacity of geologists: Upskilling course on Disaster Risk Reduction and Climate Change

An online upskilling course on Disaster Risk Reduction and Climate Change was jointly organized by The Geological Society of Malaysia (GSM), Institute of Geology Malaysia (IGM), Universiti Kebangsaan Malaysia's Southeast Asia Disaster Prevention Research Initiative (SEADPRI-UKM) and University of Malaya's Geology Department. The course, which took place on 18 December 2021 (Saturday) from 9 am-12 noon, targeted geology undergraduates from all local universities. Registration was free-of-charge on a first-come-first-served basis.

The purpose of the course was to introduce disaster risk reduction and climate change, which offers high potential for future employability of geology graduates. The course coordinator was Dr. Lin Chin Yik (UM) and lead trainers were Professor Dr. Joy Jacqueline Pereira (SEADPRI-UKM) and Dr. Nurfashareena Muhamad (SEADPRI-UKM).

The course comprised three major topics. The first topic was on concept and terminologies associated with disaster risk reduction and climate change. This was followed by a snapshot of the contribution of geoscience in building disaster and climate resilience. The final topic was on the policy dimension of disaster risk reduction and climate change. This topic covered the Sendai Framework for Disaster Risk Reduction 2015-2030, Paris Agreement 2015 and Glasgow Climate Pact 2021, as well as National Policies and Commitments of Malaysia.

A total of 18 undergraduates from University of Malaya and Universiti Malaysia Sabah attended the course. About half of them were in their final year while others were from years one to three. A post-course survey revealed that all the course participants thought that the course was very well organized. Over 94% were of the view that the presentation material was relevant and substantial with appropriate examples; interactions were fair and equitable with constructive response from the trainers. Over 80% of the participants found the presenters effective, clear and concise with interactions that sustained their interest. Overall, the participants found the course to be very helpful; several even suggested that the course be embedded as part of their curriculum. The coordinator and trainers would like to express their appreciation to Dr. Ng Tham Fatt (UM) for his guidance and Mr. Navakanesh Batmanathan (SEADPRI-UKM) for the technical support

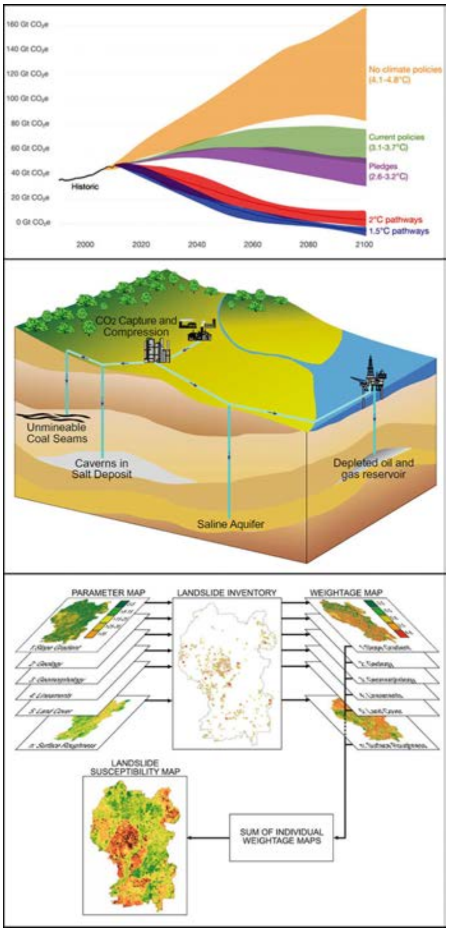

Source of graphics: Pereira J.J., Ng T.F., Hunt J. (2021), Climate Action. In: Gill J.C., Smith M. (eds.), Geosciences and the Sustainable Development Goals. Sustainable Development Goals Series. Springer, Cham. pp. 313-337, https://doi.org/10.1007/978-3-030-38815-7_13.

Prepared by Dr. Nurfashareena Muhamad (SEADPRI-UKM), Dr. Lin Chin Yik (UM) and Joy Jacqueline Pereira (SEADPRI-UKM).

LAPORAN REPORT

Courtesy visit by GSM President to IGM-GSM Sarawak Chapter

Date: 31 March 2022
Venue: Kuching, Sarawak

GSM President, P.Geol. En. Ahmad Nizam Hassan, F.I.G.M. paid a courtesy visit to IGM-GSM Sarawak Chapter led by P.Geol. Dr. Richard Mani Banda, F.I.G.M. on 31st March, 2022. He was accompanied by the Chairman of Board of Geologists Malaysia, Dato' Zakaria Mohamad, P.Geol. F.I.G.M., and IGM President, P.Geol. Gs. Abd. Rasid Jaapar, F.I.G.M. The IGM-GSM Sarawak Chapter was established in August 2021 which aimed to oversee and manage the activities or program towards the development and recognition of geoscience in Sarawak. A discussion was held during the visit to discuss on the geoscience profession direction and opportunities in Sarawak. Among other issues that have been discussed is the main event that will be implemented in Sarawak this year.

Prepared by:
P.Geol. James Bachat, M.I.G.M.
Secretary, IGM-GSM Sarawak Chapter

The GSM President presenting a gift from GSM to the Chairman of IGM-GSM Sarawak Chapter.

NEW MEMBERSHIP

Student Membership

1. Ahmad Abdillah Adnan
2. Ahmad Rashid Mohamed Yazid
3. ‘Aliyah ‘Aqilah Azmi
4. Aryo Dwi Handoko
5. Awangku Akmal Ariff Awang Ariffin
6. Castor Luis Mejos
7. Chia Kean Wei
8. Chong Siew Ting, Michelle
9. Farhan Ashley Henry
10. Grisel Paola J Soto
11. Isaac Abraham Jeslis
12. Jennytah Julimin
13. Jessie Asyura Yick
14. Ketty Freddy
15. Linckorn Dorin Boging
16. Maathumeera Rakasegaran
17. Maha Letchummy Balasingam
18. Merlissa Nurfarahin Ab Rizal
19. Messy Elbert
20. Mohamad Azri Dawisani
21. Mohammad Azim Kharudin
22. Mohammad Hairie Md Johan
23. Mohammad Shahmiezan Ridzuan
24. Mohd Fahami Sazali
25. Mohd Noor Iman
26. Muhamad Amerul Mat Aron
27. Muhammad Adhwa Fathir Muhammad Firdaus
28. Muhammad Azhar Saminoon @ Saminggun
29. Muhammad Azimuddin Mat Rahim
30. Muhammad Irfan Nizam
31. Muhammad Niqmatullah Nazmi
32. Muhammad Noor Syahfiq Suyono
33. Noor Diana Sabdalleh
34. Noralyaa Syuhada Md Zain
35. Nur Adriana Wahid
36. Nur Aqeelah Ajman
37. Nur Arifudin Nur Shidi
38. Nur Athirah Wahidah Ali
39. Nur Ezwani Eddie
40. Nur Fatin Hani Sjiaola
41. Nur Syafiqah Rahman
42. Nur Zakira Imana Mohammad Fadly
43. Nurul Amiera Nadia Khairul Fitri
44. Nurul Hamizah Muhammad Rezel
45. Ollearry Chai
46. Qalisha Maisarah Shaharudin
47. Ros Amirah Mohd Alamin
48. Shahrul Ismadi
49. Shanisha Irdyani Zainal
50. Siti Norasyikin Laning
51. Siti Nur Aimie Fitri Che Ibrahim
52. Siti Nurmasturina Shohailly
53. Slez MC Hitterson Jonaidi
54. Tan Siaw Gi
55. Teh Yu Xuan
56. Ummi Umairah Taufik
57. Vishnuvartini Rasaya

Full Membership

1. Abd Majid Sahat
2. Mohd Razani Zakaria
3. Mohd Razif Salleh
4. Nur Rashidah Abdul Aziz
5. Shinthurathi Myandran
6. Soo Khok Ping
7. Wan Mohd Nazrullah

From Student To Full Membership

1. Ahmad Zuhairi Tusiman
2. Mohamad Fairus Hj Mohamad Talhah
3. Muhamad Ngafifi Md Lahuri
4. Muhammad Taqiuddin Zakaria
5. Nurazlin Abdullah

From Full To Life Membership

1. Aimie Aisyah Othman
2. Faridah Hanim Abu Bakar
3. Khairul Azlan Mustapha
4. Kong Sher-Rine
5. Mohammad Yasir Mohd. Said
6. Mohd Rizal Lai
7. Muhammad Anasrullah Abd Rahim
8. Muhammad Fuad Razali
9. Sheila Rozalia Abdul Rashid
10. Suraya Hilmi Hazim
11. Umi Amira Jamaluddin
12. Wan Mohamed Nizam Wan Isa
13. Zaitul Zahira Ghali @ Ghazali

GSM-UMS Geology Club program

KOTA KINABALU – On January 15, 2022, the GSM-UMS Geology Club has organized an online talk, entitled 'Geotalk 9.0: Discovering the Hidden Gems – The Mining Industry'. This programme was participated by the students with geology background from University Malaysia Sabah (UMS). Panelists invited are the alumni of geology program of UMS, Mr. Edwin James and En. Shafitri Awang Kechil, who are now working in the mining industry. This program was held to help students acknowledge the opportunities and job-scope of a geologist in the mining industry.

Poster of Geotalk 9.0: Discovering the Hidden Gems – The Mining Industry. Photo by: kelabgeologi_ums on Instagram

Screenshot images of the participants of the programme on January 15, 2022. Photo by: kelabgeologi_ums on Instagram

In addition, GSM-UMS Geology Club has also hosted the Geonight Programme of Session 21/22 on 21 January, 2022 that took place in Horizon Hotel, Kota Kinabalu. This programme was held to celebrate the outgoing year 4 members that are graduating this year. At the same time, this programme has given opportunity to the organizing committee in polishing their skills in event management. Safety measures such as limiting the number of attendees and following the standard operating procedures are practiced to obey the guidelines set by Kementerian Kesihatan Malaysia.

Poster of Geonight Programme
Photo by: kelabgeologi_ums on Instagram

Photographs taken during Geonight Programme. Photo by: Isaac Abraham Jeslis

Lastly, all of the programmes were carried out smoothly, with positive feedbacks from the participants. We truly want to host more interactive and beneficial geology-related programmes in the future in conjunction with GSM and GSM-UMS Geology Club. Thank you very much.

Wong Yee Huey,
Vice Secretary

Hari Interaksi Kelab Geologi UKM

Hari Interaksi Kelab Geologi merupakan sebuah program hari keluarga anjuran Kelab Geologi Universiti Kebangsaan Malaysia, UKM yang melibatkan pelajar-pelajar geologi UKM. Objektif program ini dilaksanakan adalah untuk merapatkan hubungan silaturahim antara pelajar junior dan senior bagi menggalakkan perkongsian pengalaman dan ilmu antara satu sama lain. Program tersebut telah diadakan pada 22 Januari 2022 sekitar jam 9.00 pagi hingga 3.30 petang di Pantai Cahaya Negeri, Port Dickson, Negeri Sembilan. Seramai 31 orang peserta telah mengikuti program ini.

Program ini dimulakan dengan aktiviti berkumpulan iaitu membina rupa bumi menggunakan pasir pantai. Setiap kumpulan tersebut terdiri daripada pelajar junior dan senior yang saling bekerjasama untuk menyelesaikan misi permainan tersebut. Setelah itu, para peserta memasuki sesi rehat, jamuan makan tengah hari iaitu barbeque yang disediakan sendiri oleh ahli jawatankuasa yang bertugas. Aktiviti gotong-royong kemudian dilaksanakan secara beramai-ramai dalam kalangan peserta dan ahli jawatankuasa atas tujuan bagi memastikan lokasi pantai yang digunakan dalam keadaan baik dan bersih. Seterusnya, sesi sembang santai pelajar bersama seorang pensyarah geologi UKM iaitu Dr. Mohd Hariri bin Arifin yang merupakan penasihat program ini turut diadakan dan aktiviti ini merupakan aktiviti terakhir program. Semasa sesi ini, Dr. Hariri banyak berkongsi pengalaman serta nasihat yang bermanfaat kepada para pelajar. Berikut disertakan beberapa gambar aktiviti yang telah dijalankan semasa program berlangsung:

Laporan disediakan oleh: Alya Batrisya binti Mohd Zeffry (Setiausaha Projek)

Gambar 1: Aktiviti membina rupa bumi menggunakan pasir pantai secara berkumpulan.

Gambar 2: Penyediaan jamuan makan tengah hari (barbeque).

Gambar 3: Aktiviti gotong-royong, mengutip sampah dan mengemas peralatan program.

Gambar 4: Sesi sembang santai pelajar bersama pensyarah geologi.

Gambar 5: Perbincangan pelajar senior bersama pensyarah, Dr. Mohd Hariri bin Ariffin.

Gambar 6: Sesi bergambar semua peserta dan ahli jawatankuasa bersama penasihat program.

UPCOMING EVENTS

May 19-20, 2022: AAPG/PESGB Energy Transition Forum; London. Details are available at https://energytransition.aapg.org/2022/.

June 20-22, 2022: Unconventional Resources Technology Conference (URTeC); George R. Brown Convention Center in Houston, Texas. Visit event website https://urtec.org/2022/ for more information.

June 20-22, 2022: GeoConvention 2022 Hybrid Event; Calgary, Canada. Find more details at https://geoconvention.com/.

June 29-30, 2022: Asia Pacific E & P Conference; London. More details at event website: https://asiapacific.pesgb.org.uk/.

July 15-17, 2022: 4th International Conference on Performance-based Design in Earthquake Geotechnical Engineerin; Beijing, China. Check event website: http://www.pbd-iv2021.com/ for further details.

July 27-28, 2022: 2nd Oil, Gas and Power Cambodia; Phnom Penh. Visit www.ogpcambodia.com for information regarding this event.

August 21-24, 2022: 9th International Conference on Geoscience Education (IX GeoSciEd); in Shimane, Japan. Further information about the event can be found at https://www.geoscied9.org/.

August 28 - September 2, 2022: The International Meeting for Applied Geoscience & Energy (SEG/AAPG IMAGE '22), Houston, Texas. Visit event website: https://www.imageevent.org/ for details.

August 29 - 30, 2022: Central Australian Basins Symposium IV - "Exploring Australia's Resource Frontier"; Darwin, Australia. Contact for information: cabs@pesa.com.au or visit event website: https://agentur.eventsair.com/cmspreview/cabsiv/.

September 12-14, 2022: MEDiNA Conference and Exhibition (Mediterranean and North Africa Conference); Tunis, Tunisia. Please visit event organiser's website at https://medinace.aapg.org/2022/ for more details.

September 14-15, 2022: Lithium, Battery and Energy Metals Conference; Perth, Australia. Link for the conference: https://www.ausimm.com/conferences-and-events/lithium/program/call-for-abstracts/.

September 19-23, 2022: International Conference on Physical Modelling in Geotechnics; KAIST, Daejeon, Korea. Please check https://icpmg2022.org/ to learn more about event.

February 28 – March 2, 2023: International Petroleum Technology Conference (IPTC); Bangkok, Thailand. Available link for further details: https://2023.iptcnet.org/call-for-papers.

Geological Society of Malaysia Publications

Instruction to Authors

General Policy

Papers should be as concise as possible. They may include original results of basic, applied and policy research of national or international significance, current reviews, or discussions on techniques, research programs, organisations, information, or national and international policies in geoscience.

Submission of Papers

Only papers that have not been published elsewhere (except those in the form of abstracts, published lectures or academic theses), including electronically, will be considered for publication. Authors must agree not to publish elsewhere the submitted or accepted articles in the same form, in English, Malay or other languages. Originality detection services may be used to check your manuscript to verify its originality.

All papers will be subjected to review by two or more reviewers. Authors wishing to include published and unmodified figures or text passages are required to obtain permission from the copyright owner(s). Authors of English papers are strongly urged to have their manuscript edited for language before submission by a person whose first language is English.

The Editor reserves the right to reject all or any part of the paper submitted. The Geological Society of Malaysia assumes no responsibility for statements made by authors.

The paper should be submitted to:

The Editor,
Geological Society of Malaysia
c/o Department of Geology
University of Malaya
50603 Kuala Lumpur,
Malaysia
Tel: (603) 7957 7036
Fax: (603) 7956 3900
Email: geologicalsociety@gmail.com

Manuscript

The paper can be written in Bahasa Malaysia (Malay) or English. For English papers, use either British or American spelling but not a combination of both. The paper should be checked thoroughly for spelling and grammar. The manuscript must be printed at 1.5 spacing in a single column on one side of A4 paper. All pages should be numbered. Length of paper should be between 3,000 and 8,000 words for the Bulletin and between 2,000 and 3,000 words for Warta Geologi, excluding tables and illustrations. Metric units should be used and all non-standard symbols, abbreviations and acronyms must be defined.

Title

Title must be informative and reflects the content of the paper. Title in Malay should include an English translation. It should be concise (less than 20 words). Avoid using abbreviation in the title.

Author's Address

Addresses of all authors must be provided. The addresses should be sufficient for correspondence. Please include email address, telephone and fax of the corresponding author.

Abstract

Abstract should not exceed 300 words. Articles written in Malay language should also be accompanied by English language abstracts and keywords.

Keywords

Please include 3 to 8 keywords that best describe the content of the paper.

References

In the text, references should be cited by author and year and listed chronologically (e.g. Smith, 1964; Jones et al., 1998; Smith & Tan, 2000). For both Malay and English paper, all references must be listed in English. Title of non-English articles should be translated to English.

The list of references should only include articles cited in the text. The list should be arranged in alphabetical order. Please ensure that the reference list is complete and the bibliographical details are accurate. The references should be in the following manner:

Journal article:

Suntharalingam, T., 1968. Upper Palaeozoic stratigraphy of the area west of Kampar, Perak. Geol. Soc. Malaysia Bull., 1, 1-15.

Book:

Hutchison, C.S., 1989. Geological Evolution of South-east Asia. Clarendon Press, Oxford. 368 p.

Chapter of book and Symposium volume:

Hosking, K.F.G., 1973. Primary mineral deposits. In: Gobbett, D.J. and Hutchison, C.S. (Eds.), Geology of the Malay Peninsular (West Malaysia and Singapore). Wiley-Interscience, New York, 335-390.

Article in Malay:

Lim, C.H. & Mohd. Shafeea Leman, 1994. The occurrence of Lambir Formation in Ulu Bok Syncline, North Sarawak. Geol. Soc. Malaysia Bull., 35, 1-5. (in Malay with English abstract)

Tables

All tables should be cited in the text and numbered consecutively. Tables should have a title and a legend explaining any abbreviation or symbol used. Each table must be printed on a separate piece of paper. Do not insert the tables within the text. Data in tables should be aligned using tab stops rather than spaces. Avoid excessive tabulation of data.

Illustrations

Please make sure that all illustrations are useful, necessary and of good quality. A maximum of ten (10) illustrations (photographs, graphs and diagrams) are allowed and these should be cited in the text and numbered consecutively as Figures. The papers are usually published in black-and-white but it may sometimes be possible to include colour figures at the author's expense. The scales for maps and photomicrographs should be drawn on the figure and not given as a magnification. Originals should not be greater than A4 size and annotations should be capable of being reduced down to 50 percent. The caption should be listed on a separate piece of paper. Do not insert the illustration within the text.

Submission of Electronic Files

Authors are required to submit electronic files in a CD-ROM or email as attachments. The submission should be accompanied with a listing of all files and the software (name and version) used. The file names should reflect the content of the files (e.g. Ali_Fig1.tif). Please make sure that the files and the hardcopies are the same.

Preferred Software

Text: Microsoft Word. Do not insert tables and illustration within the text.

Tables: Microsoft Word or Microsoft Excel. Please submit as separate files.

Illustrations – Vector Graphics: Adobe Illustrator (preferred), CorelDraw and Freehand. Final line thickness should be at least 0.5 point or 0.17 mm. For other software, please submit one copy in the native file format and export one copy as a PDF file with all fonts embedded and one copy as a high resolution TIFF or JPEG image.

Photographs or bitmap (raster) images: Adobe Photoshop. Please save as TIFF or PSD files. Save/scan line art at 600 to 1200 dpi and greyscale figures at 300 to 600 dpi. High resolution JPEG, TIFF or GIF files from other sources are also acceptable. The resolution must be high enough for printing at 300 dpi.

PP2509/07/2013(032786) ISSN 0126-5539; e-ISSN 2682-7549

WARTA GEOLOGI PERSATUAN GEOLOGI MALAYSIA

Jilid 48, No. 1 • Volume 48, No. 1 • April 2022

KANDUNGAN (CONTENTS)

Published by the GEOLOGICAL SOCIETY OF MALAYSIA
Department of Geology, University of Malaya, 50603 Kuala Lumpur, MALAYSIA
Tel: 603-7957 7036 Fax: 603-7956 3900 E-mail: geologicalsociety@gmail.com

Printed by Nets Printwork Sdn. Bhd., No. 56, Jalan PBS 14/4,
Taman Perindustrian Bukit Serdang, 43300 Seri Kembangan, Selangor